Design Oriented Approach to Predict Shear Strength of Reinforced Concrete Beams

Hadi Baghi[1], Joaquim A. O. Barros[2]

[1] Post-doc, Civil Engineering and Construction Engineering Technology, Louisiana Tech University, Ruston, U.S., 71272-0046, e-mail: hadibaghi@gmail.com (corresponding author).

[2] Full Professor, ISISE, Department of Civil Engineering, University of Minho, Guimarães, Portugal, e-mail: barros@civil.uminho.pt.

Abstract

There are different approaches to predict the shear strength of reinforced concrete (RC) beams, but their predictive performance is still relatively low due to several and complex resisting mechanisms involved in shear. In addition, most of design approaches ignore the influence of the flange of T cross section beams on the ultimate shear capacity. This paper aims to present a design oriented approach to predict the load carrying capacity of RC beams failing in shear. This approach is based on the simplified modified compression field theory (SMCFT). A sensitivity analysis is carried out to assess the importance of the input parameters that mostly affect the shear strength of RC members. Taking into account the results of the sensitivity analysis, two simple equations are proposed for obtaining the: i) tensile stress factor in the cracked concrete (β); ii) inclination of the diagonal compressive stress in the web of the section (θ). The obtained equations eliminate the iterative process required by the SMCFT, and provide a straightforward design methodology to find β and θ with suitable accuracy for design purposes. In addition, a coefficient is presented to take into account the effect of the flange on the shear capacity of T shape cross section beams. To appraise the predictive performance of the new approach, a data base composed of 349 RC beams is set according to available shear tests of RC beams in literature. This data base includes beams of different size, concrete compressive strength, and longitudinal and transverse steel reinforcement ratios. By evaluating the ratio between the experimental results and the analytical predictions, an average value of 1.24 with a coefficient of variation of 20.9% is obtained, which indicate the developed model has suitable accuracy to predict the shear strength of RC beams.

Keywords: Reinforced concrete beams; Shear strength; Simplified Modified Compression Field Theory; Sensitivity Analysis; Monte Carlo simulation; T cross section beams.

Introduction

There are different methods to predict the shear strength of reinforced concrete (RC) beams, but their accuracy is still relatively low due to several and complex resisting mechanisms involved such as: concrete in the compression zone, aggregate interlock, dowel effect of longitudinal reinforcement, and contribution of stirrups if present [1, 2]. Beam's cross section dimensions and axial load, if existing, also influence the shear capacity of RC beams. The ACI Building Code [3] suggests that the nominal shear strength V_n of a RC beam is the sum of the contribution provided by concrete (V_c):

$$V_c = 0.17\sqrt{f_c'}\, b_w d \tag{1}$$

with the contribution of web reinforcement (V_s):

$$V_s = \frac{A_{st} f_{st,y}}{s} d \tag{2}$$

In equation (1) f_c' is the concrete compressive strength, while b_w and d are the width and effective depth of the beam's cross section, respectively. In equation (2) A_{st} and $f_{st,y}$ are the cross sectional area and the yield stress of steel stirrups, and s is the horizontal distance between steel stirrups. The V_s is null if transverse reinforcement is not present in the RC beam.

In the ACI Building Code [3] it is assumed the critical diagonal crack (CDC) is inclined at an angle of 45 degree. However, data from shear tests performed on RC beams with and without web reinforcement indicate that the CDC inclination depends of several mechanism involved in shear [4], thus the ACI model gives, in general, conservative estimates of shear strength for RC members, mainly when the CDC inclination is less than 45 degree.

The Modified Compression Field Theory (MCFT) was developed by Vecchio and Collins [5]. The MCFT was applied to 102 tested panels and an average ratio between experimental and model results of 1.01, with a coefficient of variation (COV) of 12.2%, was obtained [6]. Solving the equations of the MCFT to evaluate the shear capacity of a RC member requires an iterative procedure and the knowledge of a relatively high number of parameters, thus Bentz *et al.* [6] proposed a simplified approach of the MCFT, abbreviated by SMCFT. The SMCFT takes into account the tensile stress factor in the cracked concrete (β), and the inclination of the diagonal compressive stress in the web of the section (θ) to find the shear strength of a section. This model was applied to the same previous 102 RC specimens and an average ratio of experimental to the analytically predicted shear strength ($V_{exp.}/V_{ana.}$) of 1.11, with a COV of

13.0%, were obtained. In spite of the simple format of the equations for β and θ, this model still requires an iterative procedure that introduces extra difficulties in the design perspective.

Recently, Baghi and Barros [7] developed a new method based on the SMCFT and Bianco *et al.* approach [8] to predict the shear capacity of typical building RC beams shear strengthened according to the near surface mounted (NSM) technique with fiber reinforced polymer (FRP) laminates. This model takes into account the relevant features of the interaction between NSM FRP systems and surrounding concrete, like debonding of FRP laminate/rod and fracture of concrete surrounding the FRP, by considering the inclination of the CDC [9]. In the proposed model, abbreviated by SBBB, two simple equations were proposed for determining directly β and θ. This model was applied to a data base composed of 140 beams and an average value of 1.11 with COV of 14.3% were obtained for the $V_{exp.}/V_{ana.}$ ratio. However, the proposed model provided accurate predictions in RC beams with geometric and material properties in the following intervals: $170 < d < 800$ mm, $2.4 < a/d < 4.0$, $15 < f_c^{'} < 80$ MPa, $1.0\% < \rho_{sl} < 3.0$ %, $0.0 < \rho_{st} + \rho_f < 1.4\%$, where ρ_{sl} and ρ_{st} are the flexural and transverse reinforcement ratio of existing steel bars, respectively, while ρ_f is the shear strengthening ratio provided by FRP systems. The interval of these variables are representative of typical RC building beams, but the level of accuracy of this model is not known if applied to beams with relatively high cross section, typical of bridge girders.

The research about the shear resistance of T cross section beams is relatively limited, and most of the proposed models ignore the favorable effect of the flange for their shear capacity. Bresler and MacGregor [10] indicated that the shear is initiated by the formation of diagonal cracks developing in the shear span, and flexural cracks always form before the occurrence of the diagonal cracks in rectangular, I or T cross section beams. They also showed that the shear capacity and the cracks propagation are influenced by the shape of the section (I and T section) due to different magnitude of shearing stress developed in the web. However, international codes, such as ACI Building Code [3] and Eurocode [11], neglect the influence of the flange in T cross section beams, and the shear force in RC T-beams is assumed to be carried only by the web.

This paper aims to propose a design oriented approach capable of predicting with acceptable predictive performance the shear capacity of rectangular and T cross shape RC beams. For this purpose, a sensitivity analysis is carried out for assessing the relative importance of each input parameter that affects the shear capacity of RC beams according to the SMCFT. Based on the results, equations for obtaining β and θ without any iterative procedure are derived. In

addition, based on the results in literature, a parameter is proposed to predict the influence of the flange of the T cross section beams on their shear capacity. To assess the predictive performance of the proposed model, a data base (DB) composed of 349 RC beams is set, and the model's performance is appraised. The results obtained with the proposed approach are compared to the ones determined with ACI, SMCFT, and SBBB model.

Simplified Modified Compression Field Theory [6]

According to the SMCFT, the shear capacity of a RC beam (v) is obtained by the following equation:

$$v = v_c + v_s = \beta.\sqrt{f_c'} + \rho_{st}.f_{st,y}.\cot\theta \tag{3}$$

where v_c and v_s are the shear strength provided by concrete and transverse steel reinforcement, respectively, and ρ_{st} is:

$$\rho_{st} = \frac{A_{st}}{b_w.s} \tag{4}$$

In equation (3), β is the tensile stress factor in the cracked concrete, and θ is the inclination of the diagonal compressive stress in the web of the beam's cross section, which are obtained from the following respective equations:

$$\beta = \frac{0.4}{1+1500\varepsilon_{sl}}\frac{1300}{1000+s_{xe}} \tag{5}$$

$$\theta = \left(29+7000\varepsilon_{sl}\right)\left(0.88+\frac{s_{xe}}{2500}\right) \le 75° \tag{6}$$

where

$$s_{xe} = \frac{35s_x}{a_g+16} \ge 0.85s_x \tag{7}$$

represents physically the crack spacing, being s_x the vertical distance between longitudinal reinforcement, while a_g is the maximum dimension of aggregates. If the longitudinal reinforcement is not yielded, the axial strain of the longitudinal reinforcement, ε_{sl}, can be obtained from the following equation:

$$\varepsilon_{sl} = \frac{f_{sl}}{E_{sl}} = \frac{v\cot\theta - v_c/\cot\theta}{E_{sl}\rho_{sl}} \tag{8}$$

where E_{sl} is the modulus of elasticity of the longitudinal reinforcement.

The solution procedure to calculate the shear strength of a concrete beam, according to the SMCFT, is based on the following steps:

Step 1: Input parameters (E_{sl} , ρ_{sl} , $f_c^{'}$, ρ_{st} , $f_{st,y}$, a_g , $\varepsilon_{sl,y}$, and s_x);

Step 2: Calculate the crack spacing using equation (7);

Step 3: Assume a value for ε_{sl} ;

Step 4: Calculate β and θ using equations (5) and (6), respectively.

Step 5: Calculate the shear strength based on equation (3).

Step 6: Calculate the longitudinal strain, ε_{sl} , according to equation (8).

Step 7: Evaluate the normalized absolute difference between the strain values for the longitudinal reinforcement obtained in Steps 3 and 6 divided by the yield strain of the longitudinal reinforcement, $\left| \varepsilon_{sl}^{q+1} - \varepsilon_{sl}^{q} \right| / \varepsilon_{sl,y}$.

Step 8: If the value obtained in Step 7 is less than a certain adopted tolerance the iterative procedure is concluded, otherwise is return to Step 3 with the ε_{sl} determined in Step 6, and this process is executed up to obtain convergence.

More information about this method can be found in [6, 9].

SBBB model [7]:

In the SBBB model the shear strength of a RC beam is obtained according to equation (3), but β and θ are determined by the following equations:

$$\beta_s = -0.14 \times x_s^{0.21} + 0.13 \times y_s^{0.15} \qquad 0.052 < \beta_s < 0.36 \tag{9}$$

$$\theta_s = 3.36 \times \beta_s^{-0.82} + 21.5 \qquad 29° \leq \theta_s \leq 60° \tag{10}$$

where $x_s = \left(\rho_{st} f_{st,y} \right) / f_c^{'}$ and $y_s = \left(\rho_{sl} E_{sl} \right) / f_c^{'}$. As mentioned before, this approach was calibrated exclusively for predicting the shear capacity of typical RC building beams.

Sensitivity analysis

Sensitivity analysis means to study the effect of input parameters (d , b_w , $f_c^{'}$, a_g , E_{sl} , ρ_{sl} , $\bar{\sigma}_{st} = \rho_{st} \times f_{st,y}$) on the objective function (shear capacity of RC beams, equation (3)). There are two approaches to execute sensitivity analysis: local and global sensitivity analysis. Local sensitivity analysis evaluates the objective function by changing one parameter and keeping other parameters fixed. This analysis is efficient for simple objective function, but it neglects the influence of the interaction between parameters on the objective function [12]. In the global sensitivity analysis, the objective function is evaluated by varying all the parameters simultaneously, which takes into account the influence of the interaction between parameters on the objective function [13]. Global analysis is an appropriate

option for sensitivity analysis of SMCFT due to the iterative nature and complexity of the model. Monte Carlo method can be regarded as a Global sensitivity analysis. This method is a process of running the objective function numerous times with a random selection of each input parameter simultaneously.

A sensitivity analysis is carried out to assess the relative importance of each input parameter on the shear capacity of RC beams (equation (3)) in order to figure out what are the input parameters that most affect the result. All of the input parameters are characterized by a uniform probability distribution, which means a range of possible values with the same likelihood of occurrence (Table 1).

For sensitivity analysis, equation (3) is implemented in a spreadsheet that is re-calculated 500,000 times, each time with a set of random new possible values of the input parameters. The number of samples (500,000) is adopted to cover all possible scenarios for RC beams in the built environment.

To measure the influence of each input parameter on the results of v (equation (3)), β and θ, the dimensionless coefficient of correlation

$$r = \frac{n\sum_{i=1}^{n} x_i y_i - (\sum_{i=1}^{n} y_i)(\sum_{i=1}^{n} x_i)}{\sqrt{n(\sum_{i=1}^{n} x_i^2) - (\sum_{i=1}^{n} x_i)^2} \sqrt{n(\sum_{i=1}^{n} y_i^2) - (\sum_{i=1}^{n} y_i)^2}}$$

(11)

is evaluated, where n is the number of the samples, x_i is the input parameter and y_i is the output (value of equation (3), β and θ). The r varies between -1 and +1. Positive value of r means a positive linear correlation, which indicates that the objective function (y) increases with the input parameter (x), and vice versa. A negative value of r means a negative linear correlation, which indicates a decrease of y with the increase of x, or an increase of y with a decrease of x. When r is closed to 0 it means no linear correlation, or a weak linear correlation, exists. According to this definitions, the influence of the input parameters (d, b_w, f_c', a_g, E_{sl}, ρ_{sl}, $\rho_{st} \times f_{st,y}$) on the objective function (equation (3), β and θ) are presented in Figure 1. The obtained results demonstrate, d has a negative linear correlation on the v, which means when d increases v decreases, which is a consequence of size effect [14]. The remain considered parameters have positive linear correlation on the v (apart b_w that has almost null influence), mainly ρ_{sl} and $\bar{\sigma}_{st}$, since the favorable dowel effect increases with ρ_{sl} and the contribution of steel

stirrups increases with $\bar{\sigma}_{st}$. As expected, the considered parameters have opposite linear correlation on the β and θ

.

According to the results presented in Figure 1, the relationship between β vs. $\bar{\sigma}_{st}/f_c'$ and $(\rho_{sl} \times E_{sl})/f_c' \times (b_w/d)$ for

500,000 generated samples with Monte Carlo simulation are presented in Figure 2. These results can be approximated

by a surface defined by the following equation:

$$\beta_{NBB} = 0.65 \times (-0.3 \times x^{0.5} + 0.15 \times y^{0.15}) \qquad\qquad 0.035 < \beta_{NBB} < 0.39 \qquad\qquad (12)$$

where x and y are $\bar{\sigma}_{st}/f_c'$ and $(200000 \times \rho_{sl})/f_c' \times (b_w/d)$, respectively. In this equation f_c' and $\rho_{st} \times f_{st,y}$ are in

MPa. The Sum of Squares due to Error (SSE), R-square, and Root Mean Squared Error (RMSE) for this fitted surface

are 465, 0.56, and 0.03, respectively, which indicate the good fit of the model to the generated samples. More

information about these Goodness-of-Fit Statistics can be found in [7].

The relationship between β_{NBB} and θ_{NBB} is presented in Figure 3. This relationship is defined by the following

equation:

$$\theta_{NBB} = 4 \times \beta_{NBB}^{-0.7} + 22 \qquad\qquad 28^\circ \le \theta_{NBB} \le 75^\circ \qquad\qquad (13)$$

The SSE, R-square and RMSE for this fitted curve are 730000, 0.99, and 1.2, respectively. In Figure 2 the results are

fitted for 2 variables (*x* and *y*), but in Figure 3 the results are fitted for just one variable. Hence, it is reasonable the R-

square value for β_{NBB} is not so good as the one of θ_{NBB}.

Effects of flange in T-beams

As already mentioned, most of existing models neglect the effect of flange in T cross section beams on the shear load

carrying capacity. Thamrin et al. [15] proposed a simplified equation for the T-beams without shear reinforcement.

For simulating the effect of beam's flange on the shear capacity they suggested the following coefficient:

$$\alpha = 1.0 + \frac{b.h_f}{4d^2} \qquad\qquad (14)$$

where b and h_f are the width and the thickness of the flange (Figure 4). The α is multiplied by the square root of the

concrete compressive strength. However, this coefficient gives conservative estimations of the effect of the flange for

the shear capacity of T cross section beams (Figure 5a). RILEM TC162-TDF [16] recommendations take into account

the influence of the flanges on the shear capacity of T cross section beams by introducing the following coefficient

that is multiplied by the square root of the concrete compressive strength:

$$k_f = 1 + n.(h_f / b_w).(h_f / d) \leq 1.5 \tag{15a}$$

where

$$n = (b - b_w) / h_f \leq 3 \tag{15b}$$

This equation takes into account the shaded part of the flange as shown in Figure 4a, but provides unconservative results (Figure 5b). Thus, the following equation is suggested by considering half of the shaded part of the flange for the shear contribution (Figure 4b):

$$k_{fn} = 1 + n \times 0.5 \times (h_f / b_w) \times (h_f / d) \leq 1.5 \tag{16}$$

where n is obtained by equation (15b). The contribution of the flange to the beam's shear capacity is null in beams of rectangular cross section since $b = b_w$. This coefficient affects the v_c in equation (3):

$$v = v_c + v_s = k_f . \beta_{NBB} . \sqrt{f_c'} + \rho_{st} . f_{st,y} . \cot \theta_{NBB} \tag{17}$$

Assessment of the predictive performance of the developed model

An extensive data base (DB) containing 349 RC beams failing in shear [9, 17-35] was collected from published literature to appraise the predictive performance of the developed approach. This DB includes beams of different size, longitudinal and transverse steel reinforcement ratios, concrete compressive strength, and a wide range of shear span ratio to effective depth (a/d). The collected beams have the following interval of values for the relevant model's parameters: $50 \leq b_w \leq 460$ mm; $0 \leq h_f \leq 280$ mm; $125 \leq b \leq 1450$ mm; $200 \leq d < 1370$ mm; $2.4 \leq a/d < 17.03$; $10 \leq f_c'$ <125 MPa, $0.5\% \leq \rho_{sl} <15.7$ %, and $0.0 \leq \rho_{st} \times f_{st,y} < 16.7$ MPa. The DB contains values from experiments performed on 116 beams with T cross section ($k_f > 1.0$), and 234 beams with rectangular cross section ($k_f = 1.0$). The DB includes 82 beams without shear reinforcement ($\bar{\sigma}_{st} = 0$). The sample distribution of the all collected data is presented in Figure 6.

Figure 7 represents the $V_{exp.} / V_{ana.}$ of the T cross section beams for the two scenarios in terms of considering ($w - k_f$), or not ($w - o - k_f$), the contribution of the flange for the beam's shear capacity, i.e., by taken in equation (17) the k_f according to equation (16). The average value of $(V_{exp.} / V_{ana.})_{w-o-k_f}$ is 1.36 with a COV of 17.7%, while using the new approach (herein designated by NBB) that considers the contribution of the beam's flange for the shear resistance

(equation (17)), an average value of 1.17 with a COV of 15.1% for the $(V_{exp.}/V_{ana.})_{w-k_f}$ ratio were obtained, which indicate the efficiency of the proposed model to predict the shear strength of T-cross section beams.

For the NBB, ACI [3], SMCFT [6], and SBBB [7] approaches, the obtained values of $V_{ana.}$ are compared with $V_{exp.}$ of the DB, and the values of $V_{exp.}/V_{ana.}$ ratio are included in Table 2 and represented in Figures 8 and 9. The NBB model has assured an average value of $V_{exp.}/V_{ana.}$ of 1.24 for all the 349 beams with a COV of 20.9%. The ACI model has an average value of $V_{exp.}/V_{ana.}$ of 1.42 with COV of 27.0%. The SBBB and SMCFT have an average value of 1.01 and 1.09, respectively, with COV of 25% and 27%.

The predictive performance of the adopted approaches is being detrimentally affected due to some abnormal results reported in some literature that conducted to the DB with 349 beams. Due to the suspicious that some problems have occurred in the experimental programs of these beams, the corresponding results were removed from the DB, resulting a reduced DB (RDB) of 300 beams. A RC beam was removed if:

   a)   showed poor performance in all the design models ($V_{exp.}/V_{ana.} \leq 0.85$);

   b) $a/d > 10$ (high probability of has been failed in bending);

   c) $\rho_{st} \times f_{st,y} > 5$ MPa (abnormal high percentage of transverse reinforcement, where flexural failure mode is expected to have occurred);

   d) $\rho_{sl} > 5\%$ (abnormal high percentage of longitudinal reinforcement, providing unrealistic dowel effect resisting mechanism);

   e) $k_f > 1.5$ (in order to respect the condition provided by equation (15a);

The results of the RDB are presented in Figure 10. The NBB model has assured an average value of $V_{exp.}/V_{ana.}$ of 1.25 for RDB with a COV of 19%. The ACI, SBBB and SMCFT models have an average value of $V_{exp.}/V_{ana.}$ of 1.44, 1.04, and 1.10 with COV of 24.0%, 22%, and 22%, respectively.

A modified version of the Demerit Points Classification (DPC) [36] proposed by Collins [37] is presented, where a penalty (PEN) is assigned to each range of $V_{exp.}/V_{ana.}$ parameter according to Table 3, and the performance of each approach is determined by the total of penalties (Total PEN).

According to the results included in Tables 4 and 5, the predictive performance of NBB model is better than of the other models in both DB and RDB since its total penalties is the smallest one in both scenarios, which is justified by

the larger number of predictions in the appropriate safety and conservative intervals according to the DPC (Table 3). According to Table 4, the NBB model has 329 samples in appropriate safety and conservative intervals, while ACI, SMCFT, and SBBB have 307, 290, and 260 samples, respectively. The major difference between the NBB and the other models is in extremely dangerous interval ($V_{exp.}/V_{ana.} < 0.5$), since this model does not have any sample in this interval, while ACI, SMCFT, and SBBB have 5, 6, 9 samples, respectively.

Figure 11 represents graphically the influence of the following parameters (assumed the most relevant for the shear strength of a RC beam) on the predictive performance of the NBB approach: $f_c^{'}$, b_w/d, ρ_{sl}, $\rho_{st} \times f_{st,y}$, and A_f/A_t, where A_f/A_t is the ratio between the area of the flange ($b \times h_f$) and total area of the beam's cross section. Besides the good predictive performance of the NBB approach, this figure shows that no significant trend exists with respect to the design parameters, indicating their influence is being properly considered in the proposed model.

Conclusion

This paper presented a design oriented model based on the simplified modified compression field theory (SMCFT) to predict the shear capacity of reinforced concrete (RC) beams. A global sensitivity analysis (Monte Carlo simulation) with 500,000 generated samples was carried out to assess the relative importance of each input parameter on the shear capacity of the RC beams. Based on the results of the sensitivity analysis, two simple equations were proposed to directly determine the tensile stress factor in cracked concrete (β) and the inclination of the diagonal compressive stress in the web of the section (θ). These two equations were integrated into the SMCFT equation, which was coupled with an already published analytical formulation to derive a new approach (designated by NBB) for the prediction of the shear capacity of RC beams. A coefficient was introduced to take into account the effect of the flange of a T cross section beam on its shear capacity. The obtained results indicated the efficiency of the proposed model to predict the shear strength of the T-cross section beams.

A data base composed of 349 RC beams, which according to the authors were assumed failing in shear, was set to appraise the predictive performance of the proposed model, and the results were compared to the ones provided by ACI, SMCFT, and SBBB models. By evaluating the ratio between the experimental results and the analytical predictions ($V_{exp.}/V_{ana.}$), an average value of 1.24, with a coefficient of variation (COV) 20.9% was obtained by using the NBB without any prediction in extremely dangerous interval according to Demerit Points Classification. The

average value of $V_{exp.}/V_{ana.}$ for ACI, SBBB, and SMCFT models was, respectively, 1.49, 1.01, and 1.09, with COV

of 27.0%, 25.0%, and 25.0%.

References:

1.   Baghi, H., *Shear strengthening of reinforced concrete beams with SHCC-FRP panels*. 2015, University of Minho.
2.   Belarbi, A., Zomorodian, M., Yang, G., Acun, B., *PURE SHEAR TESTS ON FRP STRENGTHENED MEMBRANE ELEMENTS*, in *Conference of Structural Failure*. 2015: Szczecin-Miedzyzdrije.
3.   ACI Committee, A.C.I., & International Organization for Standardization, *Building code requirements for structural concrete (ACI 318-08) and commentary*. 2011, American Concrete Institute.
4.   Roller, J.J., Russell, H.G., *Shear Strength of High-Strength Concrete Beams with Web Reinforcement.* ACI Structural Journal, 1990. 87(2): p. 191-198.
5.   Vecchio, F.J., Collins, M.P., *The Modified Compression-Field Theory for Reinforced Concrete Elements Subjected to Shear.* ACI Journal, 1986. 83(2): p. 219-231.
6.   Bentz, E.C., Vecchio, F.J., Collins, M.P., *Simplified Modified Compression Field Theory for Calculating Shear Strength of Reinforced Concrete Elements.* ACI STRUCTURAL JOURNAL, 2006. 103: p. 614-624.
7.   Baghi, H., Barros, J.A.O., *Design Approach to Determine Shear Capacity of Reinforced Concrete Beams Shear Strengthened with NSM Systems.* Journal of Structural Engineering, 2017. 10.1061/(ASCE)ST.1943-541X.0001793.
8.   Bianco, V., Monti, G., Barros, J.A.O., *Design formula to evaluate the NSM FRP strips shear strength contribution to a RC beam.* Composites Part B: Engineering, 2013. 56: p. 960-971.
9.   Baghi, H., Barros, A.O. Joaquim,, *New Approach to Predict Shear Capacity of Reinforced Concrete Beams Strengthened with Near-Surface-Mounted Technique.* ACI Structural Journal, 2017. 114(1): p. 137-148.
10.   Bresler, B., MacGregor, J.G.,, *Review of concrete beams failing in shear.* Journal of Structural Division (ASCE), 1967. 93(ST1): p. 343-372.
11.   British Standards Institution, *Eurocode 2: Design of Concrete Structures: Part 1-1: General Rules and Rules for Buildings*. 2001, British Standards Institution.
12.   MathWorks, *What Is Sensitivity Analysis?* 2016, MathWorks.
13.   Gilman, J.R., Brickey, R.T., and Red, M.M., *Monte Carlo Techniques for Evaluating Producing Properties.* Society of Petroleum Engineers, 1998. https://doi.org/10.2118/39926-MS.
14.   Bazant, P.Z., *Size effect on structural strength: a review.* Archive of Applied Mechanics, 1999. 69: p. 703-725.
15.   Thamrin, R., Tanjung, J., Aryanti, R., Nur, O.F., Devinus, A.,, *Shear Strength of Reinforced Concrete T-Beams without Stirrups.* Journal of Engineering Science and Technology, 2016. 11(4): p. 548-562.
16.   162-TDF, R.T., *Test and design methods for steel fiber reinforced concrete, σ-ε-design method, Final Recommendation.* Materials and Structures, 2003. 36(October 2003): p. 560-567.
17.   Dias, S.J.E., Barros, J.A.O., *Shear strengthening of RC beams with NSM CFRP laminates: Experimental research and analytical formulation.* Composite Structures, 2013. 99: p. 477-490.
18.   Chaallal, O., Mofidi, A., Benmokrane, B., Neale, K., *Embedded Through-Section FRP Rod Method for Shear Strengthening of RC Beams: Performance and Comparison with Existing Techniques.* Composites for Construction, 2011. 19: p. 374-383.
19.   De Lorenzis, L., Nanni, A., *Shear Strengthening of Reinforced Concrete Beams with Near-Surface Mounted Fiber-Reinforced Polymer Rods.* ACI Structural Journal, 2001. 98: p. 60-68.
20.   Kong, P.Y.L., Rabgan, V.,, *Shear strength of high-performance concrete beams.* ACI structural journal, 1998. 95(6): p. 677-687.
21.   Frosch, R., *Behavior of Large-Scale Reinforced Concrete Beams with Minimum Shear Reinforcement.* ACI Structural Journal, 2001. 97(6): p. 814-820.

22.	Sagaseta, J., Vollum, R.L.,, *Influence of beam cross section, loading, arrangement and aggregare type on shear strength.* Magazine of concrete research, 2011. 63(2): p. 139-155.

23.	Thamrin, R., Tanjung, J., Aryanti, R., Fitrah, O., Devinus, A.,, *Shear Strength of Reinforced Concrete T-Beam without Stirrups.* Journal of Engineering Science and Technology, 2016. 11(4): p. 548-562.

24.	Yoon, Y., Cook, W., Mitchell, D., *Minimum Shear Reinforcement in Normal, Medium, and High Strength Concrete Beams.* ACI Structural Journal, 1996. 93(5): p. 576-584.

25.	Roller, J., Russell, H.,, *Shear Strength of High-Strength Concrete Beams with Web Reinforcement.* ACI Structural Journal, 1991. 78(2): p. 191-198.

26.	Johnson, M., Ramirez, J., *Minimum Shear Reinforcement in Beams with higher Strength Concrete.* ACI Structural Journal, 1989. 86(4): p. 376-382.

27.	Reineck, K., Bentz, E., Fitik, B., Kuchma, D., Bayrak., , *ACI-DAfStb Databases for Shear Tests on Slender Reinforced Concrete Beams with Stirrups.* ACI Structural Journal, 2014. 111(5): p. 1147-1156.

28.	Hsiung, W., Frantz, G.C.,, *TRANSVERSE STIRRUP SPACING IN R/C BEAMS.* Journal of Structural Engineering (ASCE), 1984. 111(2): p. 353-362.

29.	Mphonde, A.G., *Use of Stirrup Effectiveness in Shear Design of Concrete Beams.* ACI Structural Journal, 1989. 86(5): p. 541-545.

30.	Sarsam, K.F., Al-Musawi, J.M.S., *Shear Design of High- and Normal Strength Concrete Beams with Web Reinforcement.* ACI Structural Journal, 1990. 89(6): p. 658-664.

31.	Ozcebe, G., Ersoy, U., Tankut, T., *Evaluation of Minimum Shear Reinforcement Requirements for Higher Strength Concrete.* ACI Structural Journal, 1999. 96(3): p. 361-369.

32.	Angelakos, D., Bentz, E., Collins, M.,, *Effect of Concrete Strength and Minimum Stirrups on Shear Strength of Large Members.* ACI Structural Journal, 2001. 98(3): p. 290-300.

33.	Bresler, B., Scordelis, A.C.,, *Shear Strength of Reinforced Concrete Beams.* JOURNAL OF THE AMERICAN CONCRETE INSTITUTE, 1963. 60(4): p. 51-74.

34.	Lee, J., Choi, I., Kim, S.,, *Shear Behavior of Reinforced Concrete Beams with High-Strength Stirrups.* ACI Structural Journal, 2011. 108(5): p. 620-629.

35.	Krefel, W., J., Thurston, C.W., *Studies of the Shear and Diagonal Tension Strength of Simply Supported Reinforced Concrete Beams.* ACI Structural Journal, 1966. 63(21): p. 451-476.

36.	Moraes Neto, B., Barros, J., Melo, G., *Model to Simulate the Contribution of Fiber Reinforcement for the Punching Resistance of RC Slabs.* Journal of Materials in Civil Engineering, 2014. 26(7).

37.	Collins, M.P., *Evaluation of shear design procedures for concrete structures*, A.R.p.f.t.C.t.c.o.r.c. design, Editor. 2001.

Table 1: Values characterizing the uniform probability distribution of the input parameters.

	h_w (mm)	b_w (mm)	f_c' (MPa)	a_g (mm)	E_{sl} (GPa)	ρ_{sl} (%)	(MPa)
Range of variation	200-1600	50-500	10-120	10-40	180-220	0.5-5	0-5

Table 2: Summary of experimental and analytical results applied to the DB

Beam label	b_w (mm)	d (mm)	h_f (mm)	b (mm)	a/d	f_c' (MPa)	ρ_{sl} (%)	$\rho_{st} \times f_{st,y}$	V (kN)	k_f	$\dfrac{V_{exp.}}{V_{NBB}}$	$\dfrac{V_{exp.}}{V_{SBBB}}$	$\dfrac{V_{exp.}}{V_{SMCFT}}$	$\dfrac{V_{exp.}}{V_{ACI}}$
Dias and Barros [17]														
C-R-I	180	360	100	450	2.5	39.7	2.8	0.0	124	1.21	1.36	1.11	1.11	1.79
2S-R-I	180	360	100	450	2.5	39.7	2.8	0.569	182	1.21	1.40	1.26	1.20	1.71
7S-R-I	180	360	100	450	2.5	39.7	2.8	1.512	280	1.21	1.39	1.23	1.27	1.67
4S-R-II	180	360	100	450	2.5	39.7	2.8	0.948	223	1.21	1.41	1.25	1.24	1.70
C-R-III	180	360	100	450	2.5	18.6	2.8	0	88	1.21	1.26	1.03	1.07	1.85
2S-R-III	180	360	100	450	2.5	18.6	2.8	0.566	136	1.21	1.24	1.09	1.08	1.62
4S-R-III	180	360	100	450	2.5	18.6	2.8	0.938	182	1.21	1.32	1.14	1.17	1.68
C-R-IV	180	356	100	450	2.5	31.1	2.9	0	146	1.21	1.75	1.43	1.44	2.40
2S-R-IV	180	356	100	450	2.5	31.1	2.9	0.560	189	1.21	1.56	1.39	1.34	1.96
6S-R-IV	180	356	100	450	2.5	31.1	2.9	1.284	246	1.21	1.40	1.23	1.26	1.72
C-R-V	180	360	100	450	3.33	59.4	3.1	0	126	1.21	1.18	0.97	0.94	1.48
3S-R-V	180	360	100	450	3.33	59.4	3.1	0.578	180	1.21	1.24	1.12	1.04	1.47
5S-R-VI	180	360	100	450	3.33	59.4	3.1	0.865	205	1.21	1.23	1.11	1.06	1.45
Chaallal et al. [18]														
S0-CON-I	152	350	102	508	3	25	3.7	0	81	1.29	1.17	1.00	1.00	1.79
S1-CON-I	152	350	102	508	3	25	3.7	2.030	232	1.29	1.21	1.03	1.10	1.51
S3-CON-II	152	350	102	508	3	35	3.7	1.631	195	1.29	1.11	0.97	1.00	1.39
De Lorenzis and Nanni [19]														
BV	152	356	102	508	3	31	2.4	0	91	1.29	1.28	1.09	1.11	1.78
BSV	152	356	102	508	3	31	2.4	1.003	153	1.29	1.19	1.06	1.08	1.45
Baghi and Barros [7]														
C-R-II	180	360	100	450	2.5	32.7	2.8	0	128	1.21	1.50	1.23	1.24	2.03
7S-R-II	180	360	100	450	2.5	32.7	2.8	1.395	318	1.21	1.70	1.49	1.54	2.07
Kong and Rangan [20]														
S1-1	250	292	0	250	2.5	63.6	2.8	0.893	228	1.00	1.24	1.08	1.04	1.39
S2-2	250	292	0	250	2.5	72.5	2.8	0.717	232	1.00	1.34	1.17	1.09	1.47
S2-3	250	292	0	250	2.5	72.5	2.8	0.893	253	1.00	1.34	1.17	1.12	1.48
S2-5	250	292	0	250	2.5	72.5	2.8	1.190	282	1.00	1.31	1.15	1.13	1.46
S3-1	250	297	0	250	2.49	67.4	1.66	0.638	209	1.00	1.35	1.18	1.14	1.38
S4-1	250	542	0	250	2.40	87.3	3.02	0.893	354	1.00	1.04	0.84	0.79	1.05
S4-2	250	444	0	250	2.41	87.3	2.96	0.893	286	1.00	1.00	0.84	0.79	1.04
S4-3	250	346	0	250	2.40	87.3	2.84	0.893	243	1.00	1.07	0.92	0.86	1.13
S4-4	250	292	0	250	2.50	87.3	2.80	0.893	258	1.00	1.32	1.16	1.09	1.42
S4-6	250	198	0	250	2.53	87.3	2.79	0.893	203	1.00	1.46	1.34	1.27	1.65

Beam label	b_w (mm)	d (mm)	h_f (mm)	b (mm)	a/d	f_c' (MPa)	ρ_{sl} (%)	$\rho_{st} \times f_{st,y}$	V (kN)	k_f	$\dfrac{V_{exp.}}{V_{NBB}}$	$\dfrac{V_{exp.}}{V_{SBBB}}$	$\dfrac{V_{exp.}}{V_{SMCFT}}$	$\dfrac{V_{exp.}}{V_{ACI}}$
S6-5	250	299	0	250	2.64	68.9	3.69	0.638	297	1.00	1.71	1.47	1.34	1.94
S7-1	250	294	0	250	3.3	74.8	4.5	0.597	217	1.00	1.24	1.06	0.95	1.43
S7-2	250	294	0	250	3.3	74.8	4.5	0.699	205	1.00	1.11	0.96	0.86	1.29
S7-3	250	294	0	250	3.3	74.8	4.5	0.893	246	1.00	1.22	1.05	0.97	1.42
S7-4	250	294	0	250	3.3	74.8	4.5	1.115	273	1.00	1.23	1.07	1.00	1.44
S7-5	250	294	0	250	3.3	74.8	4.5	1.275	304	1.00	1.28	1.12	1.06	1.51
S7-6	250	294	0	250	3.3	74.8	4.5	1.491	311	1.00	1.21	1.06	1.02	1.43
S8-1	250	292	0	250	2.5	74.6	2.8	0.597	272	1.00	1.66	1.44	1.33	1.80
S8-2	250	292	0	250	2.5	74.6	2.8	0.717	251	1.00	1.44	1.25	1.17	1.57
S8-3	250	292	0	250	2.5	74.6	2.8	0.893	265	1.00	1.40	1.22	1.16	1.54
S8-5	250	292	0	250	2.5	74.6	2.8	1.115	289	1.00	1.38	1.21	1.18	1.53
Frosch [21]														
V1-V2	455	838	0	455	3.0	35	0.98	0.390	391	1.00	0.76	0.62	0.63	0.73
Sagaseta and Vollum [22]														
BG01	135	465	0	135	3.46	80	1	0	62	1.00	0.84	0.52	0.77	0.65
BL01	135	465	0	135	3.46	68	1	0	50	1.00	0.72	0.45	0.80	0.57
BG1	135	437	0	135	3.52	31.7	3.32	2.695	285	1.00	1.20	0.93	1.02	1.32
BG2	135	437	0	135	3.52	31.7	3.32	4.565	322	1.00	0.93	0.70	0.81	0.99
BL1	135	437	0	135	3.52	53.11	3.32	2.695	350	1.00	1.41	1.11	1.19	1.51
BL2	135	437	0	135	3.52	53.11	3.32	4.565	478	1.00	1.32	1.03	1.17	1.40
CB1	160	437	0	160	3.52	49.35	2.80	1.925	308	1.00	1.32	1.06	1.11	1.41
CB2	160	437	0	160	3.52	49.35	2.80	2.915	429	1.00	1.39	1.11	1.22	1.49
Thamrin et al. [23]														
R-01E	125	219	0	125	3.7	32	1.0	0	33	1.00	1.28	0.88	0.93	1.25
R-02E	125	219	0	125	3.7	32	1.5	0	37	1.00	1.35	0.93	0.95	1.41
R-03E	125	212	0	125	3.8	32	2.5	0	38	1.00	1.32	0.91	0.89	1.49
T-01E	125	219	70	250	3.7	32	1.0	0	37	1.16	1.24	0.99	1.04	1.41
T-02E	125	219	70	250	3.7	32	1.5	0	39	1.16	1.23	0.98	1.00	1.48
T-03E	125	212	70	250	3.8	32	2.5	0	48	1.17	1.43	1.15	1.12	1.88
Yoon et al. [24]														
N1-S	375	655	0	375	3.28	36	2.9	0	249	1.00	0.88	0.61	0.66	0.99
N1-N	375	655	0	375	3.28	36	2.9	0.353	457	1.00	1.22	0.98	0.97	1.36
N2-N	375	655	0	375	3.28	36	2.9	0.516	483	1.00	1.14	0.93	0.88	1.28
M1-S	375	655	0	375	3.28	67	2.9	0	296	1.00	0.84	0.58	0.61	0.87
M1-N	375	655	0	375	3.28	67	2.9	0.35	405	1.00	0.92	0.74	0.71	0.95
M2-S	375	655	0	375	3.28	67	2.9	0.50	552	1.00	1.14	0.93	0.85	1.19

Beam label	b_w (mm)	d (mm)	h_f (mm)	b (mm)	a/d	f_c' (MPa)	ρ_{sl} (%)	$\rho_{st} \times f_{st,y}$	V (kN)	k_f	$\dfrac{V_{exp.}}{V_{NBB}}$	$\dfrac{V_{exp.}}{V_{SBBB}}$	$\dfrac{V_{exp.}}{V_{SMCFT}}$	$\dfrac{V_{exp.}}{V_{ACI}}$
M2-N	375	655	0	375	3.28	67	2.9	0.70	689	1.00	1.27	1.05	0.98	1.34
H1-S	375	655	0	375	3.28	87	2.9	0	327	1.00	0.85	0.58	0.61	0.84
H1-N	375	655	0	375	3.28	87	2.9	0.353	483	1.00	1.02	0.82	0.78	1.01
H2-S	375	655	0	375	3.28	87	2.9	0.600	598	1.00	1.10	0.90	0.82	1.11
H2-N	375	655	0	375	3.28	87	2.9	1.006	721	1.00	1.09	0.91	0.87	1.13
Roller and Russell [25]														
1	356	559	0	356	2.5	120	1.59	0.341	298	1.00	0.77	0.64	0.60	0.68
2	356	559	0	356	2.5	120	2.89	1.969	1098	1.00	1.37	1.19	1.19	1.44
3	356	559	0	356	2.5	120	4.4	3.939	1657	1.00	1.27	1.10	1.16	1.44
4	356	559	0	356	2.5	120	5.78	5.79	1942	1.00	1.09	0.95	1.01	1.28
5	356	559	0	356	2.5	120	6.71	8.11	2237	1.00	0.96	0.83	0.91	1.13
6	457	762	0	457	3.0	72	1.65	0.360	665	1.00	1.11	0.92	0.92	1.06
7	457	762	0	457	3.0	72	1.82	0.702	787	1.00	1.06	0.89	0.86	1.05
8	457	762	0	457	3.0	125	1.82	0.363	484	1.00	0.69	0.57	0.55	0.61
9	457	762	0	457	3.0	125	2.28	0.702	748	1.00	0.87	0.73	0.67	0.83
10	457	762	0	457	3.0	125	2.75	1.023	1172	1.00	1.16	0.98	0.92	1.15
Johnson and Ramirez [26]														
2	305	350	0	305	3.13	36	2.37	0.334	222	1.00	1.34	1.14	1.06	1.54
4	305	350	0	305	3.13	72	2.37	0.334	316	1.00	1.59	1.36	1.22	1.67
5	305	350	0	305	3.13	55	2.37	0.677	382	1.00	1.67	1.45	1.39	1.85
Reineck et al. [27]														
ET1	300	300	0	300	3.5	23.0	1.39	0.57	144.5	1.00	1.00	0.88	0.91	1.16
ET2	150	300	75	300	3.5	23.0	2.78	1.16	134.5	1.13	1.24	1.05	1.09	1.51
ET3	100	300	75	300	3.5	23.0	4.17	1.73	130.0	1.25	1.38	1.13	1.18	1.70
ET4	50	300	75	300	3.5	23.0	8.34	3.46	101.0	1.50	1.31	0.99	1.05	1.57
TA3	160	375	80	960	3.33	15.4	4.40	2.51	283	1.16	1.20	0.96	1.05	1.48
TA4	160	375	80	960	3.33	15.4	4.40	1.53	239	1.16	1.42	1.16	1.22	1.81
TA15	160	375	80	960	3.33	17.4	4.40	2.51	303	1.16	1.27	1.02	1.11	1.57
TA11	160	375	80	960	3.33	24.9	4.40	2.5	347	1.16	1.41	1.15	1.24	1.73
TA12	160	375	80	960	3.33	24.9	4.40	1.53	275	1.16	1.54	1.28	1.31	1.93
TA16	160	375	80	960	3.33	17.4	4.40	2.51	304	1.16	1.28	1.03	1.12	1.57
T1	152	254	76	610	3.36	27.9	1.25	0.58	109	1.22	1.63	1.51	1.56	1.91
T2	152	254	76	610	3.36	28.1	1.46	0.00	54.7	1.22	1.20	1.02	1.06	1.57
T3	152	254	76	610	3.36	27.5	1.46	0.58	105	1.22	1.55	1.43	1.45	1.85
T4	152	254	76	610	3.36	32.5	1.95	0.58	109	1.22	1.49	1.38	1.36	1.82
T5	152	254	76	610	3.36	33.7	1.46	1.15	140	1.22	1.46	1.33	1.43	1.70

Beam label	b_w (mm)	d (mm)	h_f (mm)	b (mm)	a/d	f_c' (MPa)	ρ_{sl} (%)	$\rho_{st} \times f_{st,y}$	V (kN)	k_f	$\dfrac{V_{exp.}}{V_{NBB}}$	$\dfrac{V_{exp.}}{V_{SBBB}}$	$\dfrac{V_{exp.}}{V_{SMCFT}}$	$\dfrac{V_{exp.}}{V_{ACI}}$
T6	152	254	76	610	3.6	25.8	4.16	2.25	205	1.22	1.33	1.15	1.22	1.71
T7	152	254	76	610	3.46	27.4	3.00	0.58	109	1.22	1.47	1.34	1.30	1.92
T8	152	254	76	610	3.60	31.3	4.16	0.58	125	1.22	1.56	1.43	1.35	2.11
T9	152	254	76	610	3.60	20.2	4.16	1.15	154	1.22	1.54	1.36	1.39	2.08
T10	152	254	76	610	3.36	28.2	1.46	0.38	87	1.22	1.46	1.37	1.35	1.76
T11	152	254	76	610	3.60	37.0	4.16	1.15	160	1.22	1.45	1.32	1.30	1.90
T12	152	254	76	610	3.60	30.7	4.16	0.58	145	1.22	1.82	1.67	1.58	2.47
T13	152	254	76	610	3.36	12.8	1.46	0.58	90	1.22	1.55	1.39	1.46	1.96
T14	152	254	76	610	3.60	33.4	4.16	2.25	219	1.22	1.38	1.21	1.27	1.75
T15	152	254	76	610	7.20	33.2	4.16	0.58	104	1.22	1.28	1.18	1.11	1.73
T16	152	254	76	610	7.20	32.7	4.16	0.38	93	1.22	1.30	1.21	1.11	1.78
T18	152	254	76	610	3.60	28.4	4.16	0.00	75	1.22	1.41	1.20	1.15	2.14
T19	152	254	76	610	5.40	30.0	4.16	0.58	113	1.22	1.43	1.31	1.24	1.94
T20	152	254	76	610	5.40	32.1	4.16	1.15	154	1.22	1.43	1.29	1.28	1.89
T22	152	254	76	610	3.36	34.4	1.46	0.58	109	1.22	1.53	1.42	1.43	1.79
T25	152	254	76	610	3.36	54.1	1.46	0.58	115	1.22	1.45	1.37	1.35	1.63
T26	152	254	76	610	3.60	57.0	4.16	1.15	179	1.22	1.51	1.38	1.33	1.91
T27	152	254	76	610	3.60	12.0	4.16	1.15	132	1.22	1.43	1.23	1.28	1.97
T31	152	254	76	610	3.36	31.0	1.46	0.58	95	1.22	1.36	1.27	1.28	1.61
T32	152	254	76	610	3.60	27.6	4.16	2.25	216	1.22	1.39	1.21	1.28	1.78
T34	152	254	76	540	5.40	43.0	4.16	0.58	112	1.22	1.30	1.20	1.11	1.71
T36	152	254	152	610	3.60	24.2	4.16	1.15	179	1.50	1.60	1.55	1.56	2.33
T37	152	254	76	610	3.60	31.8	4.16	2.25	210	1.22	1.33	1.16	1.22	1.70
T38	152	256	152	610	3.60	30.2	4.16	2.25	239	1.50	1.43	1.32	1.39	1.93
R1	152	254	0	152	3.36	26.2	0.975	0.0	44.9	1.00	1.32	0.92	0.98	1.34
R2	152	254	0	152	3.36	26.2	1.46	0.0	47.1	1.00	1.30	0.90	0.94	1.40
R3	152	254	0	152	3.36	24.8	1.46	0.0	44.9	1.00	1.27	0.88	0.91	1.37
R7	152	254	0	152	3.36	28.1	1.46	0.0	54.3	1.00	1.46	1.02	1.05	1.56
R8	152	254	0	152	3.36	26.7	1.46	0.6	79.6	1.00	1.29	1.07	1.10	1.39
R9	152	254	0	152	3.36	29.6	1.46	1.2	104.5	1.00	1.17	0.98	1.07	1.27
R10	152	254	0	152	3.36	29.6	0.975	0.6	75.2	1.00	1.26	1.06	1.11	1.28
R11	152	254	0	152	3.36	26.2	1.95	0.6	89.4	1.00	1.41	1.16	1.16	1.58
R12	152	254	0	152	3.6	33.9	4.16	0.6	109.4	1.00	1.49	1.22	1.15	1.78
R13	152	254	0	152	3.6	32.3	4.16	1.2	149.5	1.00	1.47	1.22	1.21	1.79
R14	152	254	0	152	3.36	29.0	1.46	0.4	89.4	1.00	1.67	1.37	1.36	1.76
R15	152	254	0	152	3.6	29.9	4.16	1.2	139.7	1.00	1.39	1.15	1.15	1.70

Beam label	b_w (mm)	d (mm)	h_f (mm)	b (mm)	a/d	f_c' (MPa)	ρ_{sl} (%)	$\rho_{st} \times f_{st,y}$	V (kN)	k_f	$\dfrac{V_{exp.}}{V_{NBB}}$	$\dfrac{V_{exp.}}{V_{SBBB}}$	$\dfrac{V_{exp.}}{V_{SMCFT}}$	$\dfrac{V_{exp.}}{V_{ACI}}$
R16	152	254	0	152	3.6	31.6	4.16	1.2	139.7	1.00	1.38	1.15	1.14	1.68
R17	152	254	0	152	3.36	12.8	1.46	0.6	69.8	1.00	1.30	1.06	1.12	1.50
R18	152	254	0	152	3.36	31.3	1.46	0.6	84.5	1.00	1.33	1.11	1.12	1.41
R19	152	254	0	152	3.36	30.3	1.46	1.2	119.7	1.00	1.34	1.13	1.22	1.45
R20	152	254	0	152	3.36	43.0	1.46	0.6	89.8	1.00	1.33	1.11	1.11	1.36
R21	152	254	0	152	3.6	48.0	4.16	1.2	149.5	1.00	1.39	1.16	1.13	1.63
R22	152	254	0	152	4.5	29.5	1.46	0.6	79.6	1.00	1.27	1.06	1.07	1.35
R24	152	254	0	152	5.05	30.9	4.16	0.6	92.1	1.00	1.28	1.05	0.99	1.54
R25	152	254	0	152	3.6	30.8	4.16	0.6	104.5	1.00	1.46	1.19	1.12	1.75
R27	152	254	0	152	3.6	13.7	4.16	1.2	94.7	1.00	1.04	0.85	0.88	1.34
R28	152	254	0	152	3.6	31.6	4.16	2.2	179.3	1.00	1.21	1.01	1.06	1.47
T21	110	298	80	400	3.5	33.1	3.84	1.42	132	1.29	1.35	1.16	1.18	1.68
T22	110	298	80	400	3.5	31.7	3.84	1.51	130	1.29	1.29	1.11	1.13	1.61
T23	110	298	80	400	3.5	35	3.84	1.20	142	1.29	1.57	1.37	1.36	1.96
T1a	110	298	80	400	3.5	23.4	3.84	1.53	135	1.29	1.39	1.18	1.22	1.75
T2a	110	298	80	400	3.5	25.1	3.84	1.64	139	1.29	1.36	1.15	1.20	1.70
Ta3	110	298	80	400	3.5	25.1	3.84	1.32	130	1.29	1.44	1.23	1.26	1.83
Ta4	110	298	80	400	3.5	25.7	3.84	1.37	135	1.29	1.46	1.25	1.28	1.85
T1b	110	298	80	400	3.5	23.6	3.84	1.15	120	1.29	1.45	1.24	1.26	1.85
T2b	110	298	80	400	3.5	25.4	3.84	1.23	132	1.29	1.52	1.30	1.32	1.93
T3b	110	298	80	400	3.5	25.1	3.84	0.77	118	1.29	1.70	1.49	1.46	2.22
T4b	110	298	80	400	3.5	25.2	3.84	0.82	109	1.29	1.53	1.34	1.31	1.99
T5	110	298	80	400	3.5	26	3.84	0.82	112	1.29	1.56	1.37	1.34	2.03
P5	150	285	80	600	3.5	43.0	1.45	1.07	145	1.22	1.38	1.26	1.32	1.55
P20	150	285	80	600	3.5	40.7	1.94	0.65	120	1.22	1.38	1.26	1.24	1.62
P23	150	285	80	600	3.5	43.1	1.94	1.07	160	1.22	1.47	1.33	1.37	1.71
No. 2	190	374	102	610	4.14	32.8	0.69	0.00	72	1.22	0.94	0.78	0.79	1.04
A00	190	394	102	610	3.92	32.7	0.66	0.00	65	1.21	0.83	0.67	0.65	0.89
A25	190	390	102	610	3.97	32.6	0.66	0.22	86	1.21	0.95	0.88	0.88	0.97
A25a	190	388	102	610	4.00	33.1	0.67	0.22	83	1.21	0.91	0.85	0.84	0.94
A50	190	392	102	610	3.96	26.3	0.66	0.51	115	1.21	1.07	0.97	1.05	1.12
A50a	190	393	102	610	3.94	28.0	0.66	0.51	109	1.21	1.00	0.90	0.98	1.04
A75	190	395	102	610	3.92	32.2	0.66	0.67	142	1.21	1.13	1.02	1.15	1.16
No. 1	190	371	102	610	4.18	38.1	0.70	0.76	134	1.22	1.02	0.94	1.08	1.05
B00	190	399	102	610	3.88	32.0	0.49	0.00	70	1.21	0.93	0.75	1.49	0.96
B25	190	394	102	610	3.93	30.8	0.49	0.22	79	1.21	0.92	0.85	0.90	0.91

Beam label	b_w (mm)	d (mm)	h_f (mm)	b (mm)	a/d	$f_c^{'}$ (MPa)	ρ_{sl} (%)	$\rho_{st} \times f_{st,y}$	V (kN)	k_f	$\dfrac{V_{exp.}}{V_{NBB}}$	$\dfrac{V_{exp.}}{V_{SBBB}}$	$\dfrac{V_{exp.}}{V_{SMCFT}}$	$\dfrac{V_{exp.}}{V_{ACI}}$
B50	190	391	102	610	3.96	30.6	0.50	0.53	107	1.21	0.99	0.90	1.28	0.98
C50	190	393	102	610	3.94	29.7	0.94	0.53	134	1.21	1.14	1.03	1.07	1.23
C75	190	395	102	610	3.92	29.4	0.93	0.71	138	1.21	1.04	0.93	1.00	1.13
I	50	240	65	200	10.4	40	5.23	0.00	22	1.41	1.16	0.97	0.90	1.71
III	50	240	65	200	3.33	40	5.23	0.00	37	1.41	1.95	1.63	1.51	2.87
VHA	75	704	140	585	3.41	44.5	14.5	8.87	887	1.50	1.58	1.07	1.16	1.68
HA-45	150	1369	280	1450	3.06	43.3	9.4	9.75	3384	1.50	1.57	1.00	1.14	1.52
RC 30 A1	120	940	130	900	4.04	25	8.02	4.02	682	1.22	1.13	0.79	0.85	1.24
RC 60 A1	120	940	130	900	4.04	47	9.41	4.02	938	1.22	1.43	1.05	1.09	1.60
RC 60 B1	120	940	130	900	4.04	50	12.53	6.03	1200	1.22	1.31	0.95	1.00	1.47
RC 70 B1	120	940	130	900	4.04	60	12.53	6.03	1330	1.22	1.43	1.05	1.09	1.60
2	90	647	125	500	2.56	87.4	6.13	4.06	548	1.40	1.53	1.20	1.24	1.67
3	90	647	125	500	2.56	88.3	8.98	9.60	891	1.40	1.30	0.95	1.05	1.37
4	90	661	125	500	2.50	89.3	10.81	16.67	1221	1.39	1.17	0.78	0.91	1.12
IB-2R	178	308	102	584	2.97	16.8	1.42	1.29	140	1.28	1.07	0.94	1.05	1.29
IC-1R	178	299	102	584	3.06	34.0	4.53	5.46	414	1.29	1.00	0.83	0.96	1.21
IC-2R	178	310	102	584	2.95	34.0	4.37	1.29	227	1.28	1.35	1.23	1.23	1.80
ID-2R	178	306	102	584	2.99	34.0	2.47	1.29	220	1.29	1.42	1.30	1.35	1.77
GT-2	120	350	100	500	3.46	24.9	2.99	1.21	148	1.36	1.37	1.19	1.23	1.71
GT-4	120	350	100	500	3.46	31.0	2.99	2.51	227	1.36	1.33	1.11	1.22	1.56
GT-5	120	350	100	500	3.46	19.5	2.99	3.22	222	1.36	1.16	0.91	1.06	1.33
A2	155	719	150	655	2.68	30.8	2.86	2.62	657	1.30	1.52	1.18	1.30	1.65
B2	155	719	150	655	2.68	31.4	2.86	1.96	571	1.30	1.58	1.26	1.34	1.76
Stb III	77	590	107	838	4.27	60.6	13.55	6.16	537	1.38	1.37	1.02	1.07	1.58
Stb I	77	590	100	837	4.27	60.6	15.61	9.21	682	1.33	1.29	0.92	0.98	1.43
5A-0	120	540	90	700	2.78	25.7	3.88	3.53	435	1.19	1.40	1.04	1.17	1.53
5B-0	120	540	90	700	2.78	26.6	3.88	3.39	435	1.19	1.44	1.08	1.20	1.57
DB0.530M	300	925	0	300	2.88	32	0.5	0.4	265	1.00	0.84	0.65	0.83	0.70
B1S	240	300	0	300	2.70	27.2	1.26	0.65	129	1.00	1.06	0.92	0.96	1.17
B2S	240	600	0	600	2.80	25.5	1.26	0.65	250	1.00	1.13	0.90	0.94	1.15
B3S	240	900	0	900	2.85	26.7	1.26	0.65	369	1.00	1.17	0.88	0.91	1.12
B4S	240	1200	0	1200	2.88	25.8	1.26	0.65	473	1.00	1.17	0.85	0.89	1.09
V1	175	322	0	175	3.57	38	1.07	0.70	100	1.00	1.02	0.85	0.89	1.02
VL1	120	278	63	301	3.24	43	3.01	3.07	190	1.17	1.19	0.99	1.10	1.36
RsIS/BQ II 0	250	430	125	900	3.0	24.5	3.95	4.26	595	1.22	0.90	0.74	0.85	1.08

Beam label	b_w (mm)	d (mm)	h_f (mm)	b (mm)	a/d	f'_c (MPa)	ρ_{sl} (%)	$\rho_{st} \times f_{st,y}$	V (kN)	k_f	$\dfrac{V_{exp.}}{V_{NBB}}$	$\dfrac{V_{exp.}}{V_{SBBB}}$	$\dfrac{V_{exp.}}{V_{SMCFT}}$	$\dfrac{V_{exp.}}{V_{ACI}}$
RnIIS	450	548	150	950	3.0	22.1	1.36	1.87	745	1.14	0.96	0.85	0.99	1.13
Hsiung and Frantz [28]														
A	152	419	0	152	3	43	1.82	0.62	110	1.00	1.01	0.79	0.77	1.00
B	305	419	0	305	3	43	1.82	0.62	200	1.00	0.84	0.71	0.70	0.90
C	457	419	0	457	3	43	1.82	0.62	339	1.00	0.90	0.81	0.79	1.02
Mphonde [29]														
B50-3-3	153	299	0	153	3.6	22	3.36	0.34	76	1.00	1.23	0.97	0.92	1.46
B50-7-3	153	299	0	153	3.6	40	3.36	0.34	94	1.00	1.32	1.04	0.92	1.45
B50-11-3	153	299	0	153	3.6	60	3.36	0.34	98	1.00	1.23	0.98	0.85	1.29
B50-115-3	153	299	0	153	3.6	83	3.36	0.34	111	1.00	1.28	1.01	0.87	1.28
B100-3-3	153	299	0	153	3.6	28	3.36	0.69	95	1.00	1.12	0.90	0.88	1.31
B100-7-3	153	299	0	153	3.6	59	3.36	0.69	94	1.00	0.96	0.78	0.72	1.03
B100-11-1	153	299	0	153	3.6	69	3.36	0.69	152	1.00	1.50	1.22	1.12	1.58
B100-15-3	153	299	0	153	3.6	82	3.36	0.69	116	1.00	1.10	0.89	0.82	1.14
B150-3-3	153	299	0	153	3.6	29	3.36	1.03	139	1.00	1.33	1.08	1.09	1.56
B150-7-3	153	299	0	153	3.6	47	3.36	1.03	133	1.00	1.18	0.97	0.95	1.32
B150-11-3	153	299	0	153	3.6	70	3.36	1.03	161	1.00	1.34	1.10	1.05	1.44
B150-15-3	153	299	0	153	3.6	83	3.36	1.03	150	1.00	1.21	1.00	0.94	1.27
Sarsam and Al-Musawi [30]														
AL2-N	180	235	0	180	4	10	2.23	0.76	115	1.00	1.65	1.38	1.44	2.10
AL2-H	180	235	0	180	4	75	2.23	0.76	123	1.00	1.24	1.07	1.03	1.30
AS2-H	180	232	0	180	2.5	76	2.26	0.76	201	1.00	2.04	1.77	1.65	2.15
AS3-N	180	235	0	180	2.5	40	2.23	1.14	199	1.00	1.86	1.61	1.47	2.12
AS3-H	180	235	0	180	2.5	72	2.23	1.14	199	1.00	1.70	1.48	1.10	1.82
BL2-H	180	233	0	180	4	76	2.82	0.76	138	1.00	1.36	1.17	1.61	1.47
BS3-H	180	233	0	180	2.5	73	2.82	1.14	228	1.00	1.90	1.65	1.28	2.10
BS4-H	180	233	0	180	2.5	80	2.82	1.53	207	1.00	1.46	1.28	1.14	1.62
CL2-H	180	233	0	180	4	70	3.51	0.76	147	1.00	1.44	1.23	1.31	1.61
CS3-H	180	233	0	180	2.5	74	3.51	1.14	247	1.00	2.00	1.73	1.44	2.26
CS4-H	180	233	0	180	2.5	76	3.51	1.53	220	1.00	1.53	1.33	1.03	1.74
Ozcebe et al. [31]														
ACI56	150	310	0	150	5	58	3.46	0.31	94	1.00	1.20	0.94	0.82	1.26
TH56	150	310	0	150	5	63	3.46	0.38	103	1.00	1.23	0.97	0.85	1.28
TS56	150	310	0	150	5	61	3.46	0.54	129	1.00	1.40	1.12	1.02	1.49
ACI59	150	310	0	150	5	82	4.43	0.31	97	1.00	1.09	0.85	0.71	1.13
TH59	150	310	0	150	5	75	4.43	0.42	119	1.00	1.28	1.01	0.86	1.35

Beam label	b_w (mm)	d (mm)	h_f (mm)	b (mm)	a/d	f'_c (MPa)	ρ_{sl} (%)	$\rho_{st} \times f_{st,y}$	V (kN)	k_f	$\dfrac{V_{exp.}}{V_{NBB}}$	$\dfrac{V_{exp.}}{V_{SBBB}}$	$\dfrac{V_{exp.}}{V_{SMCFT}}$	$\dfrac{V_{exp.}}{V_{ACI}}$
TS59	150	310	0	150	5	82	4.43	0.63	125	1.00	1.17	0.94	0.84	1.24
ACI36	150	310	0	150	3	75	2.59	0.31	105	1.00	1.30	1.03	0.90	1.27
TH36	150	310	0	150	3	75	2.59	0.38	141	1.00	1.67	1.33	1.17	1.64
TS36	150	310	0	150	3	75	2.59	0.54	156	1.00	1.68	1.35	1.24	1.67
ACI39	150	310	0	150	3	73	3.07	0.31	112	1.00	1.37	1.07	0.93	1.37
TH39	150	310	0	150	3	73	3.07	0.38	143	1.00	1.67	1.32	1.15	1.68
TS39	150	310	0	150	3	73	3.07	0.63	179	1.00	1.80	1.45	1.34	1.85
Angelakos et al. [32]														
DB120	300	925	0	300	2.92	21	1.01	0	179	1.00	0.86	0.55	0.67	0.83
DB130	300	925	0	300	2.92	32	1.01	0	185	1.00	0.77	0.49	0.59	0.69
DB140	300	925	0	300	2.92	38	1.01	0	180	1.00	0.70	0.45	0.53	0.62
DB165	300	925	0	300	2.92	65	1.01	0	185	1.00	0.60	0.38	0.44	0.49
DB180	300	925	0	300	2.92	80	1.01	0	172	1.00	0.52	0.33	0.36	0.41
DB230	300	895	0	300	3	32	2.09	0	257	1.00	0.98	0.63	0.73	1.00
DB0.530	300	925	0	300	2.92	32	0.5	0	165	1.00	0.76	0.48	0.36	0.62
DB0.530M	300	925	0	300	2.92	32	0.5	0.40	263	1.00	0.84	0.65	0.83	0.70
DB120M	300	925	0	300	2.92	21	1.01	0.40	282	1.00	0.89	0.68	0.70	0.86
DB140M	300	925	0	300	2.92	38	1.01	0.40	277	1.00	0.77	0.59	0.59	0.69
DB165M	300	925	0	300	2.92	65	1.01	0.40	452	1.00	1.10	0.85	0.91	0.92
DB180M	300	925	0	300	2.92	80	1.01	0.40	395	1.00	0.91	0.70	0.74	0.74
B100	300	895	0	300	3	36	1.01	0	225	1.00	0.92	0.59	0.70	0.82
B100HE	300	925	0	300	2.92	98	1.01	0	217	1.00	0.61	0.39	0.39	0.46
B100L	300	925	0	300	2.92	39	1.01	0	223	1.00	0.86	0.55	0.65	0.76
BN100	300	925	0	300	2.92	37	0.76	0	192	1.00	0.79	0.50	0.60	0.67
BH100	300	925	0	300	2.92	99	0.76	0	193	1.00	0.56	0.36	0.19	0.41
BRL100	300	925	0	300	2.92	94	0.5	0	163	1.00	0.52	0.33	0.20	0.36
BM100	300	925	0	300	2.92	47	0.76	0.40	342	1.00	0.94	0.73	0.80	0.79
Bresler and Scordelis [33]														
OA-1	310	461	0	310	3.97	27	1.81	0.00	167	1.00	1.17	0.83	0.89	1.32
OA-2	305	466	0	305	4.9	34	2.27	0.00	178	1.00	1.13	0.79	0.83	1.26
OA-3	307	462	0	307	6.94	48	2.74	0.00	189	1.00	1.03	0.73	0.74	1.13
A-1	307	466	0	307	3.92	27	1.8	0.33	234	1.00	1.22	1.01	0.97	1.35
A-2	305	464	0	305	4.93	34	2.28	0.33	245	1.00	1.19	0.97	0.93	1.31
B-1	231	461	0	231	3.95	27	2.43	0.48	222	1.00	1.37	1.10	1.06	1.53
B-2	229	466	0	229	4.91	34	2.43	0.48	200	1.00	1.18	0.94	0.90	1.27
C-1	155	464	0	155	3.95	27	1.8	0.65	156	1.00	1.37	1.06	1.07	1.41

Beam label	b_w (mm)	d (mm)	h_f (mm)	b (mm)	a/d	f_c' (MPa)	ρ_{sl} (%)	$\rho_{st} \times f_{st,y}$	V (kN)	k_f	$\dfrac{V_{exp.}}{V_{NBB}}$	$\dfrac{V_{exp.}}{V_{SBBB}}$	$\dfrac{V_{exp.}}{V_{SMCFT}}$	$\dfrac{V_{exp.}}{V_{ACI}}$
C-2	152	464	0	152	4.93	34	3.66	0.66	162	1.00	1.27	0.97	0.92	1.39
Lee et al. [34]														
S20-1	250	300	0	250	2.5	25	2.7	1.45	187	1.00	0.89	0.76	0.80	1.08
S20-2	250	300	0	250	2.5	25	2.7	1.67	201	1.00	0.87	0.75	0.80	1.06
S20-3	250	300	0	250	2.5	25	2.7	1.90	221	1.00	0.88	0.75	0.82	1.07
S20-4	250	300	0	250	2.5	25	2.7	2.25	252	1.00	0.89	0.76	0.84	1.08
S30-1	300	520	0	300	4	33	2.92	0.00	190	1.00	1.09	0.75	0.79	1.25
S30-3	300	520	0	300	4	33	2.92	0.87	300	1.00	0.90	0.75	0.74	1.04
S30-4	300	520	0	300	4	33	2.92	0.87	311	1.00	0.94	0.77	0.76	1.08
S30-5	300	520	0	300	4	33	2.92	1.74	447	1.00	0.90	0.75	0.79	1.05
S35-1	250	300	0	250	2.5	35	2.7	1.45	226	1.00	1.03	0.89	0.93	1.23
S35-2	250	300	0	250	2.5	35	2.7	1.67	245	1.00	1.02	0.89	0.93	1.22
S35-3	250	300	0	250	2.5	35	2.7	1.90	258	1.00	0.99	0.86	0.92	1.18
S35-4	250	300	0	250	2.5	35	2.7	2.25	254	1.00	0.87	0.75	0.82	1.04
S40-1	300	369	0	300	2.76	38	4.65	0.00	176	1.00	1.20	0.87	0.85	1.52
S40-2	300	369	0	300	2.76	38	4.65	1.89	398	1.00	0.97	0.84	0.86	1.22
S40-3	300	369	0	300	2.76	38	4.65	2.42	537	1.00	1.11	0.96	1.00	1.40
S40-4	300	369	0	300	2.76	38	4.65	2.78	567	1.00	1.07	0.92	0.97	1.34
S40-5	300	369	0	300	2.76	38	4.65	3.17	592	1.00	1.01	0.87	0.94	1.27
S40-6	300	369	0	300	2.76	38	4.65	3.75	491	1.00	0.74	0.64	0.70	0.92
S50-1	300	369	0	300	2.76	50	4.65	0.00	187	1.00	1.15	0.84	0.81	1.41
S50-2	300	369	0	300	2.76	50	4.65	1.89	587	1.00	1.39	1.21	1.22	1.71
S50-3	300	369	0	300	2.76	50	4.65	2.42	641	1.00	1.30	1.13	1.16	1.60
S50-4	300	369	0	300	2.76	50	4.65	2.78	657	1.00	1.21	1.05	1.10	1.49
S50-5	300	369	0	300	2.76	50	4.65	3.17	710	1.00	1.19	1.03	1.10	1.47
S50-6	300	369	0	300	2.76	50	4.65	3.75	759	1.00	1.13	0.98	1.05	1.38
S80-1	300	369	0	300	2.76	81	4.65	0.00	262	1.00	1.37	0.99	0.93	1.55
S80-2	300	369	0	300	2.76	81	4.65	1.89	668	1.00	1.49	1.31	1.28	1.76
S80-3	300	369	0	300	2.76	81	4.65	2.42	723	1.00	1.39	1.22	1.23	1.65
S80-4	300	369	0	300	2.76	81	4.65	2.78	784	1.00	1.38	1.21	1.24	1.64
S80-5	300	369	0	300	2.76	81	4.65	3.17	838	1.00	1.35	1.19	1.23	1.61
Krefeld and Thurston [35]														
26-1	254	456	0	254	8.03	40	2.22	0.54	207	1.00	1.03	0.84	1.11	1.11
29b-1	254	456	0	254	8.03	38	2.22	0.37	160	1.00	0.91	0.74	0.99	0.97
213.5-1	254	456	0	254	8.03	39	2.22	0.24	148	1.00	0.93	0.74	0.99	0.98
29a-2	254	456	0	254	8.03	37	2.22	0.43	217	1.00	1.19	0.97	1.29	1.28

Beam label	b_w (mm)	d (mm)	h_f (mm)	b (mm)	a/d	f_c' (MPa)	ρ_{sl} (%)	$\rho_{st} \times f_{st,y}$	V (kN)	k_f	$\dfrac{V_{exp.}}{V_{NBB}}$	$\dfrac{V_{exp.}}{V_{SBBB}}$	$\dfrac{V_{exp.}}{V_{SMCFT}}$	$\dfrac{V_{exp.}}{V_{ACI}}$
29b-2	254	456	0	254	8.03	41	2.22	0.43	202	1.00	1.08	0.88	1.16	1.15
29c-2	254	456	0	254	8.03	24	2.22	0.43	161	1.00	0.98	0.79	1.11	1.10
29d-2	254	456	0	254	8.03	30	2.22	0.43	165	1.00	0.95	0.77	1.05	1.05
29e-2	254	456	0	254	8.03	48	2.22	0.43	206	1.00	1.06	0.86	1.12	1.11
29g-2	254	456	0	254	8.03	16	2.22	0.43	150	1.00	0.99	0.80	1.17	1.17
213.5a-2	254	456	0	254	8.03	37	2.22	0.29	161	1.00	0.99	0.79	1.07	1.05
218a-2	254	456	0	254	8.03	38	2.22	0.21	164	1.00	1.07	0.85	1.14	1.13
29-3	254	456	0	254	8.03	34	2.22	0.28	178	1.00	1.13	0.90	1.22	1.21
318-1	254	456	0	254	8.03	41	2.22	0.64	220	1.00	1.02	0.84	1.11	1.10
321-1	254	456	0	254	8.03	39	2.22	0.54	164	1.00	0.82	0.67	0.89	0.88
318-2	254	456	0	254	8.03	39	2.22	0.44	177	1.00	0.95	0.77	1.03	1.02
321-2	254	456	0	254	8.03	38	2.22	0.38	167	1.00	0.95	0.77	1.02	1.01
313.5-3	254	456	0	254	8.03	43	2.22	0.45	214	1.00	1.12	0.91	1.20	1.18
318-3	254	456	0	254	8.03	43	2.22	0.33	175	1.00	1.00	0.81	1.06	1.05
321-3	254	456	0	254	8.03	43	2.22	0.29	141	1.00	0.83	0.67	0.88	0.87
4A3	203	390	0	203	4.69	31	2.06	0	110	1.00	1.36	0.92	1.44	1.47
11A2	152	314	0	152	5.83	30	3.41	0	73	1.00	1.41	0.95	1.57	1.64
12A2	152	238	0	152	7.69	30	4.5	0	64	1.00	1.51	1.06	1.81	1.90
18A2	152	316	0	152	5.79	19	2.68	0	63	1.00	1.48	0.99	1.68	1.77
18B2	152	316	0	152	5.79	20	2.68	0	72	1.00	1.66	1.11	1.89	1.97
18C2	152	316	0	152	5.79	23	2.68	0	73	1.00	1.60	1.08	1.82	1.86
18D2	152	316	0	152	5.79	22	2.68	0	60	1.00	1.34	0.90	1.50	1.57
13A2	152	319	0	152	5.73	20	0.8	0	48	1.00	1.31	0.88	1.35	1.30
14A2	152	243	0	152	7.53	21	1.05	0	35	1.00	1.14	0.80	1.26	1.22
15A2	152	316	0	152	5.79	20	1.34	0	46	1.00	1.18	0.79	1.26	1.26
15B2	152	316	0	152	5.79	21	3.14	0	52	1.00	1.15	0.77	1.32	1.39
16A2	152	240	0	152	7.62	22	1.77	0	42	1.00	1.26	0.88	1.44	1.44
17A2	152	243	0	152	7.53	22	2.09	0	44	1.00	1.27	0.89	1.49	1.49
18E2	152	316	0	152	5.79	20	2.68	0	82	1.00	1.89	1.27	2.15	2.25
19A2	152	240	0	152	7.62	21	3.53	0	46	1.00	1.26	0.88	1.58	1.62
20A2	152	238	0	152	7.69	21	4.52	0	51	1.00	1.36	0.95	1.68	1.81
21A2	203	238	0	203	7.69	20	5.01	0	77	1.00	1.47	1.08	1.92	2.10
2AC	152	254	0	152	9.6	23	1.32	0	38	1.00	1.12	0.78	1.23	1.21
3AC	152	256	0	152	9.54	21	1.99	0	44	1.00	1.25	0.86	1.48	1.45
4AC	152	254	0	152	9.6	16	2.63	0	38	1.00	1.14	0.79	1.40	1.45
5AC	152	252	0	152	9.66	18	3.35	0	42	1.00	1.18	0.82	1.46	1.52

Beam label	b_w (mm)	d (mm)	h_f (mm)	b (mm)	a/d	f_c' (MPa)	ρ_{sl} (%)	$\rho_{st} \times f_{st,y}$	V (kN)	k_f	$\dfrac{V_{exp.}}{V_{NBB}}$	$\dfrac{V_{exp.}}{V_{SBBB}}$	$\dfrac{V_{exp.}}{V_{SMCFT}}$	$\dfrac{V_{exp.}}{V_{ACI}}$
6AC	152	250	0	152	9.74	23	4.3	0	53	1.00	1.32	0.92	1.67	1.71
3CC	152	256	0	152	11.92	20	1.99	0	36	1.00	1.04	0.72	1.21	1.22
4CC	152	254	0	152	12	21	2.63	0	40	1.00	1.09	0.76	1.36	1.33
5CC	152	252	0	152	12.07	20	3.35	0	44	1.00	1.19	0.83	1.50	1.51
6CC	152	250	0	152	12.17	21	4.3	0	44	1.00	1.13	0.79	1.48	1.49
4EC	152	254	0	152	14.4	21	2.63	0	42	1.00	1.15	0.80	1.41	1.40
5EC	152	252	0	152	14.48	19	3.35	0	40	1.00	1.10	0.76	1.38	1.41
6EC	152	250	0	152	14.6	19	4.3	0	42	1.00	1.12	0.78	1.48	1.49
4GC	152	254	0	152	16.8	21	2.63	0	37	1.00	1.01	0.70	1.25	1.23
5GC	152	252	0	152	16.9	22	3.35	0	42	1.00	1.10	0.76	1.39	1.38
6GC	152	250	0	152	17.03	21	4.3	0	40	1.00	1.03	0.72	1.36	1.35
Ave											1.24	1.01	1.09	1.42
SD											0.26	0.25	0.27	0.38
COV											20.9	25.0	25.0	27.0

Table 3: Demerit points classification criteria

$V_{exp.}$ / $V_{ana.}$	Classification	Penalty
<0.5	Extremely Dangerous	10
[0.5-0.85[	Dangerous	5
[0.85-1.15[	Appropriate Safety	0
[1.15-2[	Conservative	1
≥2.0	Extremely Conservative	2

Table 4: Predictive performance of different approaches according to the modified version of the DPC on DB

$V_{exp.}$ / $V_{ana.}$	NBB		SBBB		SMCFT		ACI	
	N^o samples	Total	N^o samples	Total	N^o samples	Total	N^o samples	Total
<0.5	0	0	9	90	6	60	5	50
[0.5-0.85[	18	90	80	300	52	260	19	95
[0.85-1.15[	106	0	156	0	153	0	63	0
[1.15-2[	223	223	104	104	137	137	244	244
≥ 2.0	2	4	0	0	1	2	18	36
$\sum$ PEN	349	317	349	494	349	459	349	425

Table 5: Predictive performance of different approaches according to the modified version of the DPC on RDB

$V_{exp.}$ / $V_{ana.}$	NBB		SBBB		SMCFT		ACI	
	Nº samples	Total	Nº samples	Total	Nº samples	Total	Nº samples	Total
<0.5	0	0	0	0	0	0	0	0
[0.5-0.85[	4	20	62	310	44	220	10	50
[0.85-1.15[	95	0	141	0	136	0	61	0
[1.15-2[	199	199	97	97	119	119	214	214
≥ 2.0	2	4	0	0	1	2	15	30
∑ PEN	300	223	300	407	300	341	300	294

Figure Caption List

Figure 1: Sensitivity analysis for: a) SMCFT model; b) the tensile stress in the cracked concrete (β); and the inclination of the diagonal compressive stress in the web of the section (θ)

Figure 2: The relation between β_{NBB} *vs.* $\dfrac{\bar{\sigma}_{st}}{f_c'}$ and $\dfrac{\rho_{sl} \times E_{sl}}{f_c'} \times (\dfrac{b_w}{d})$
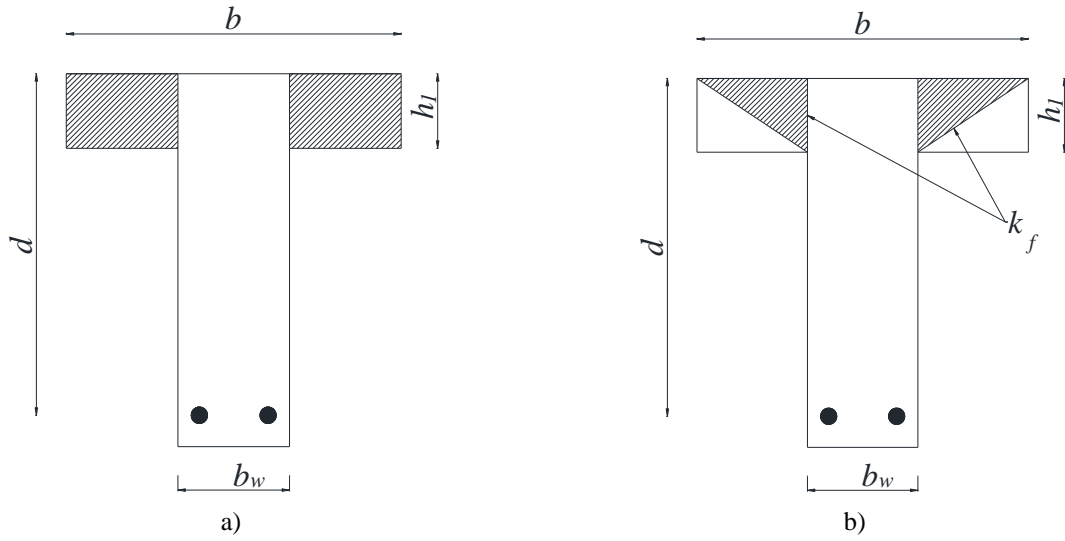
Figure 3: Relation between θ_{NBB} and β_{NBB}

Figure 4: Area of T-cross section beam considered in: a) RILEM TC162-TDF [14] recommendations (equation (15)), b) equation (16)

Figure 5: Effects of flange on the load carrying capacity according to Thamrin et al. [13] and RILEM TC162-TDF [14] recommendation.
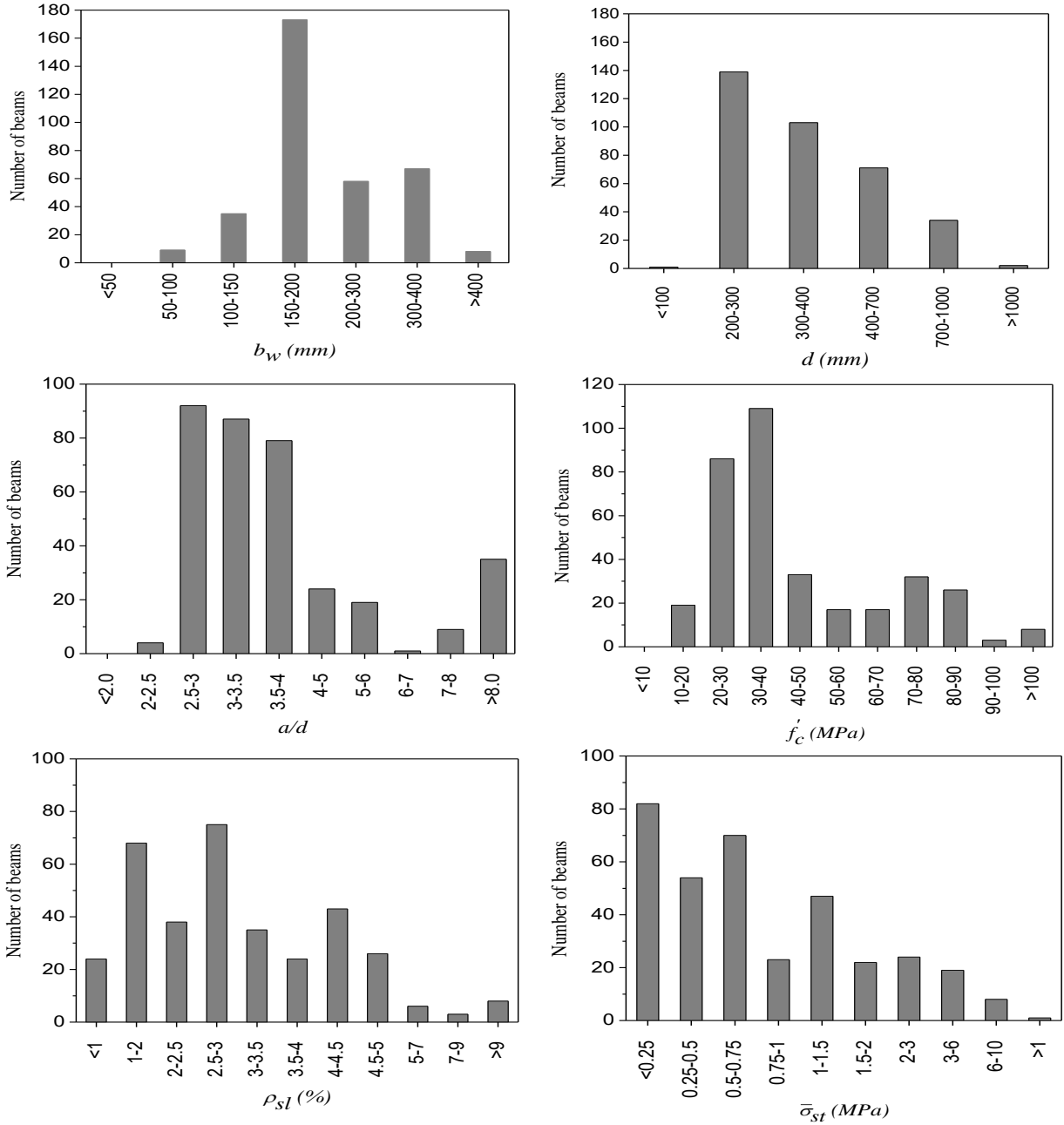
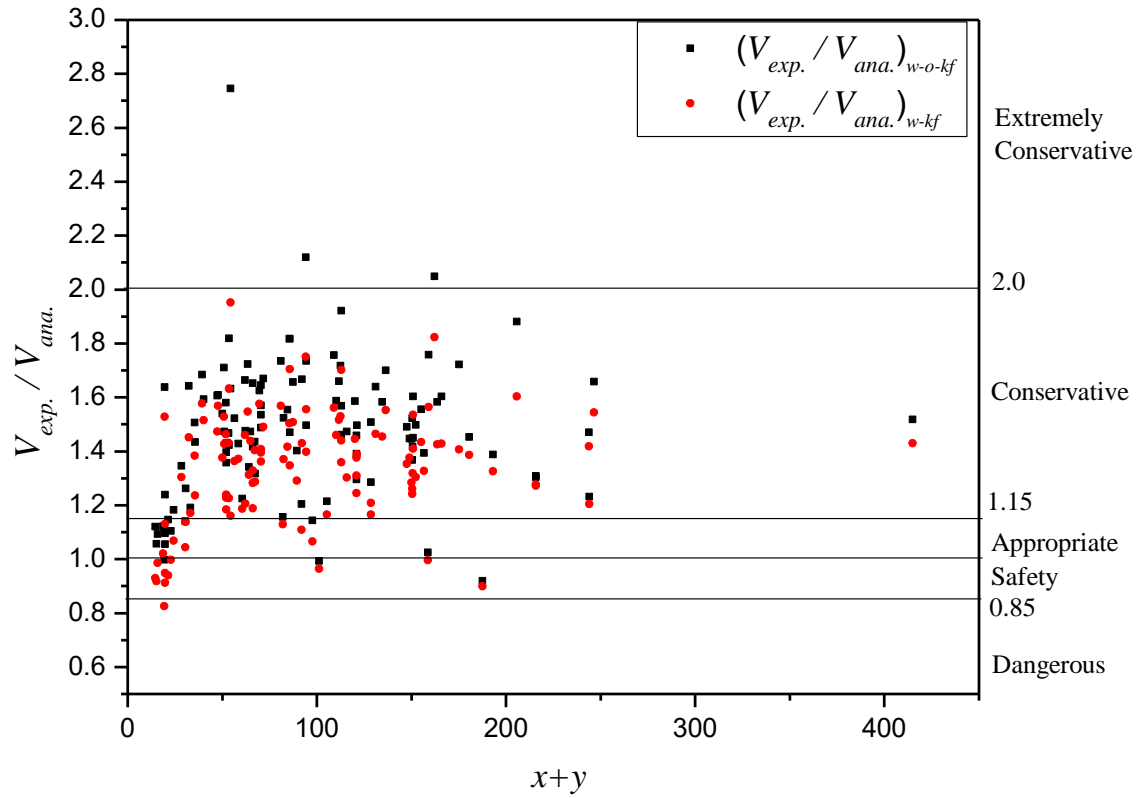Figure 6: Distribution of the variables used in data base (DB)

Figure 7: Values of the experimental *vs.* analytical ratio for the T-cross section beams of the data base ($x + y = \dfrac{\bar{\sigma}_{st}}{f_c'} + \dfrac{200000 \times \rho_{sl}}{f_c'} \times (\dfrac{b_w}{d})$)
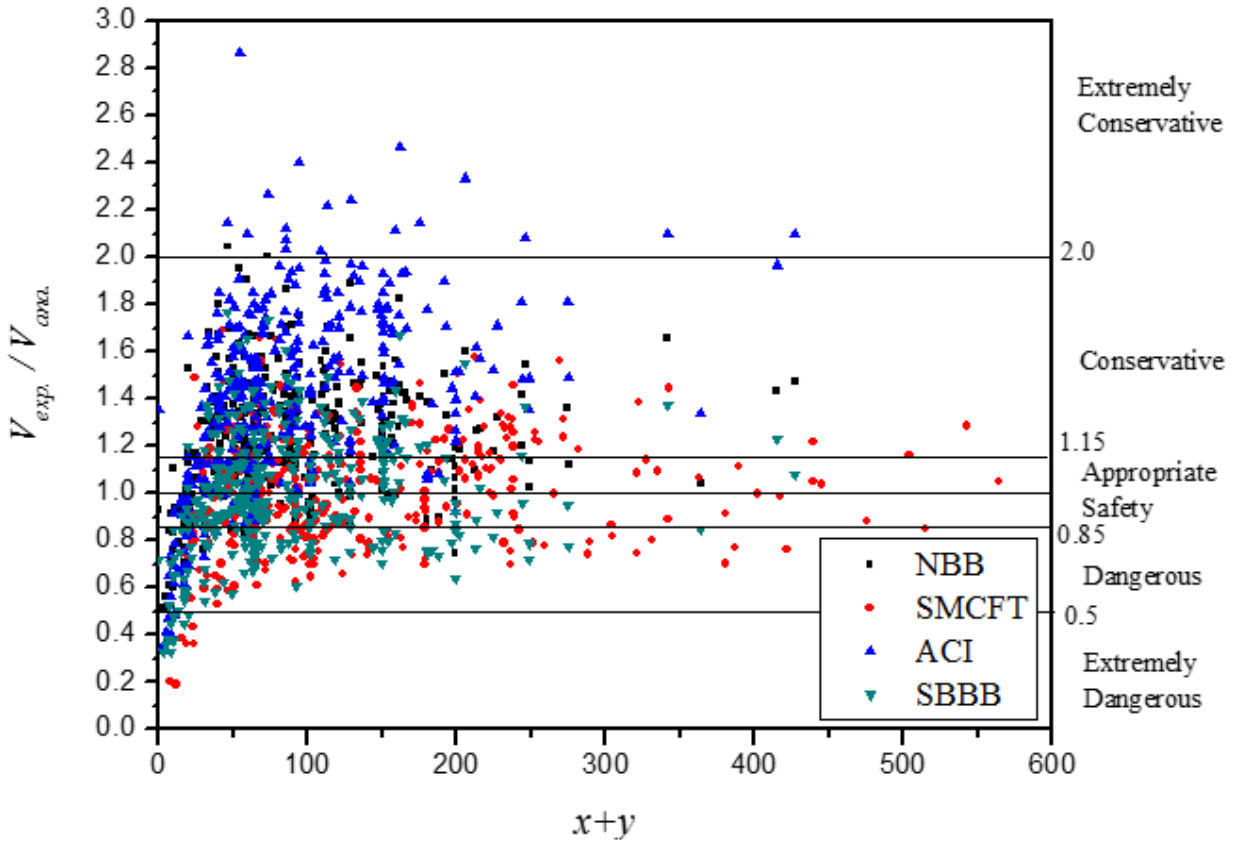
Figure 8: Values of the experimental *vs.* analytical ratio for the analyzed approaches, considering the results from the collected data base ($x + y = \dfrac{\bar{\sigma}_{st}}{f_c'} + \dfrac{200000 \times \rho_{sl}}{f_c'} \times (\dfrac{b_w}{d})$)
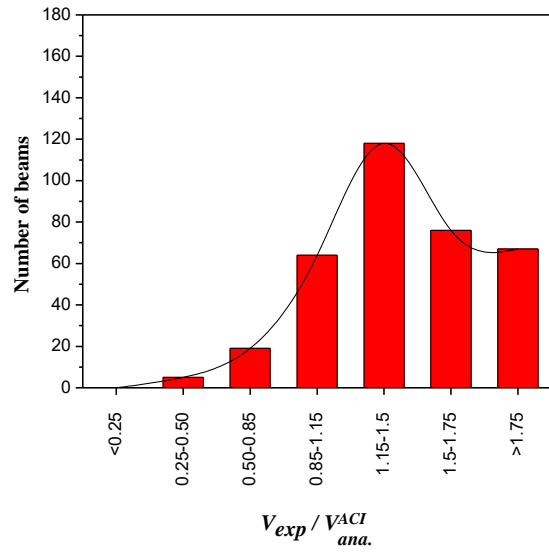
Figure 9: Distribution of the results for different models.

Figure 10: Values of the experimental *vs.* analytical ratio, considering the results from the RDB

Figure 11: The ratio between the predicted and experimental shear strength values with respect to the f_c', d, ρ_{sl}, $\bar{\sigma}_{st}$, b_w, and A_f / A_t

Figure 1: Sensitivity analysis for: a) SMCFT model; b) the tensile stress in the cracked concrete (β); and the inclination of the diagonal compressive stress in the web of the section (θ)
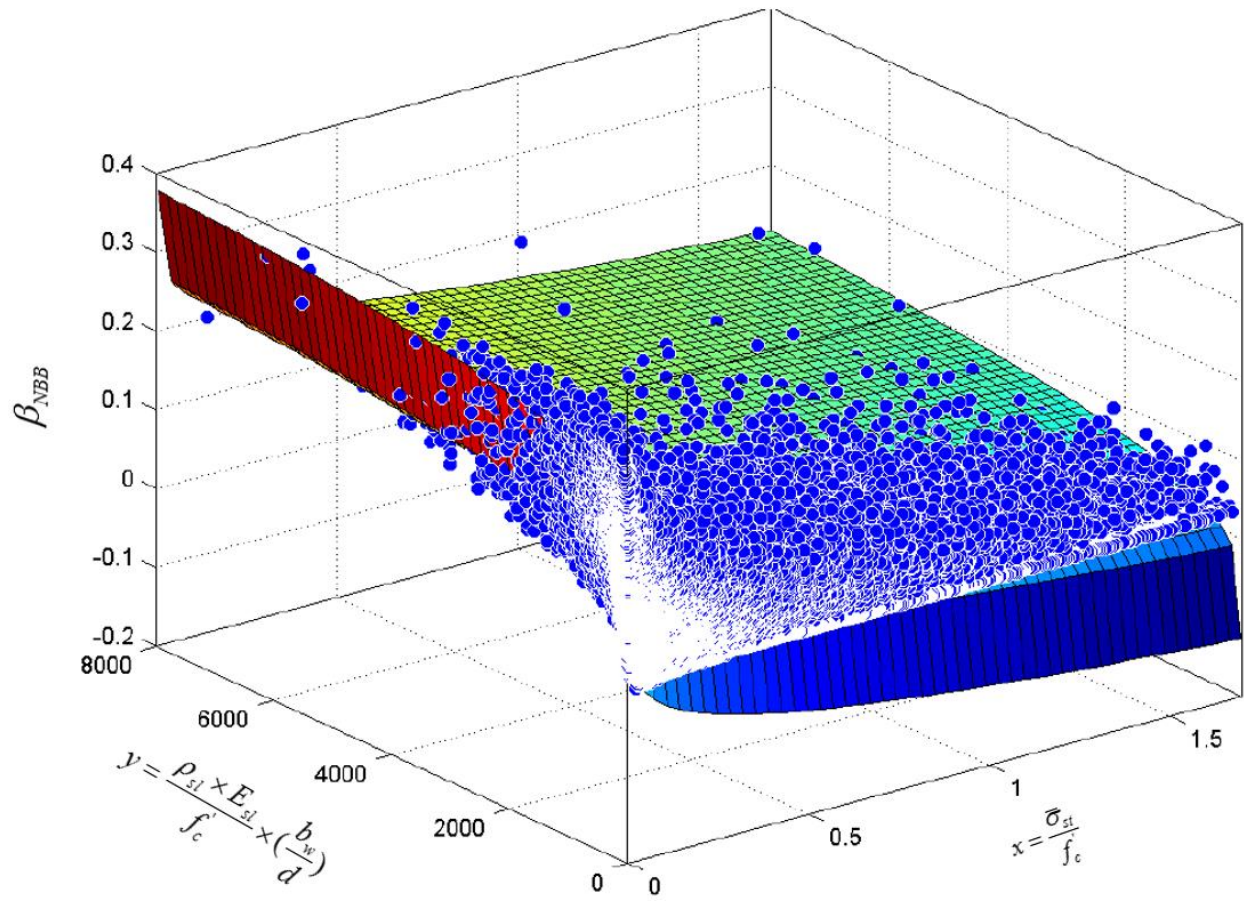
Figure 2: The relation between β_{NBB} vs. $\dfrac{\overline{\sigma}_{st}}{f_c^{'}}$ and $\dfrac{\rho_{sl} \times E_{sl}}{f_c^{'}} \times (\dfrac{b_w}{d})$
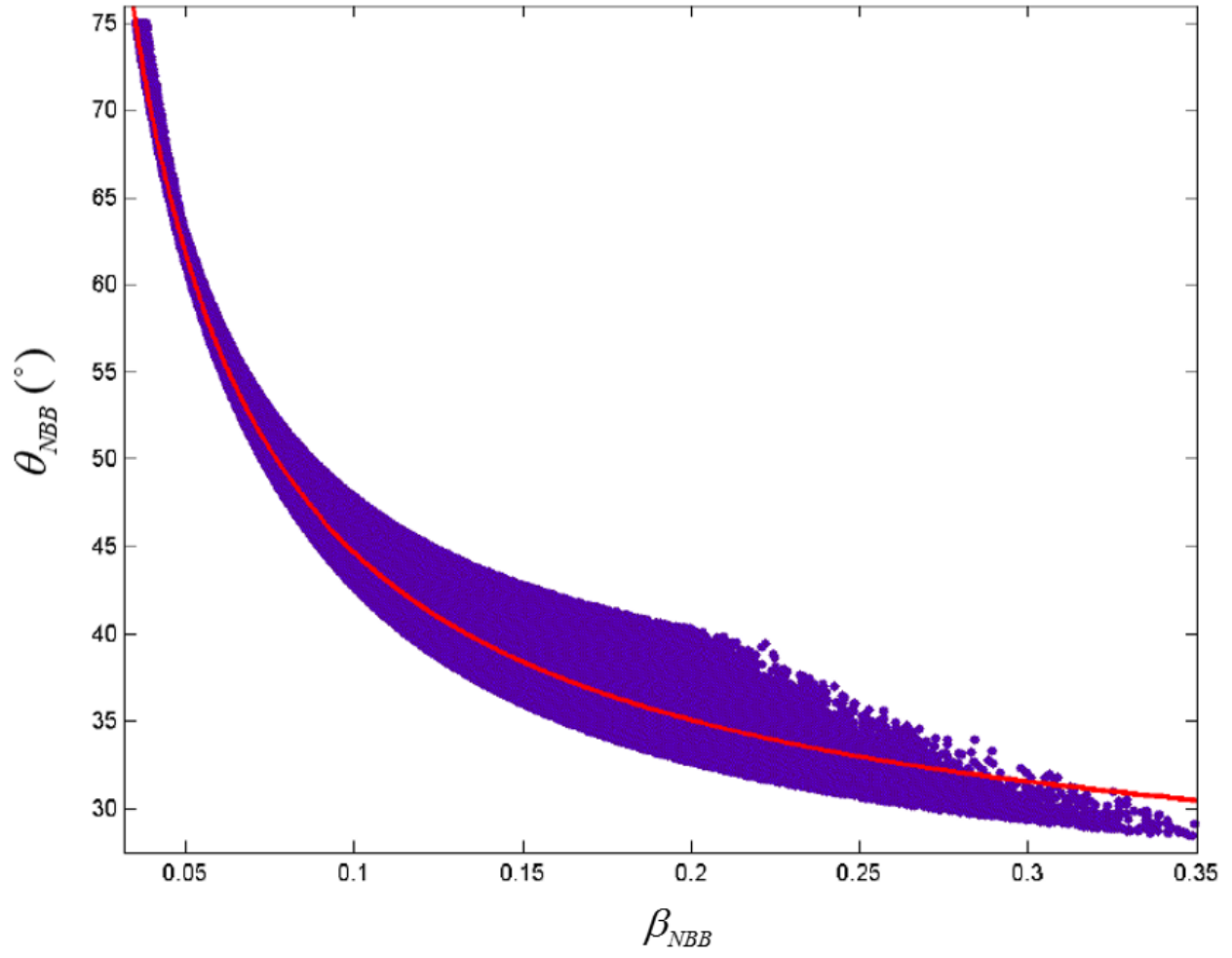
Figure 3: Relation between θ_{NBB} and β_{NBB}

Figure 4: Area of T-cross section beam considered in: a) RILEM TC162-TDF [14] recommendations (equation (15)), b) equation (16)
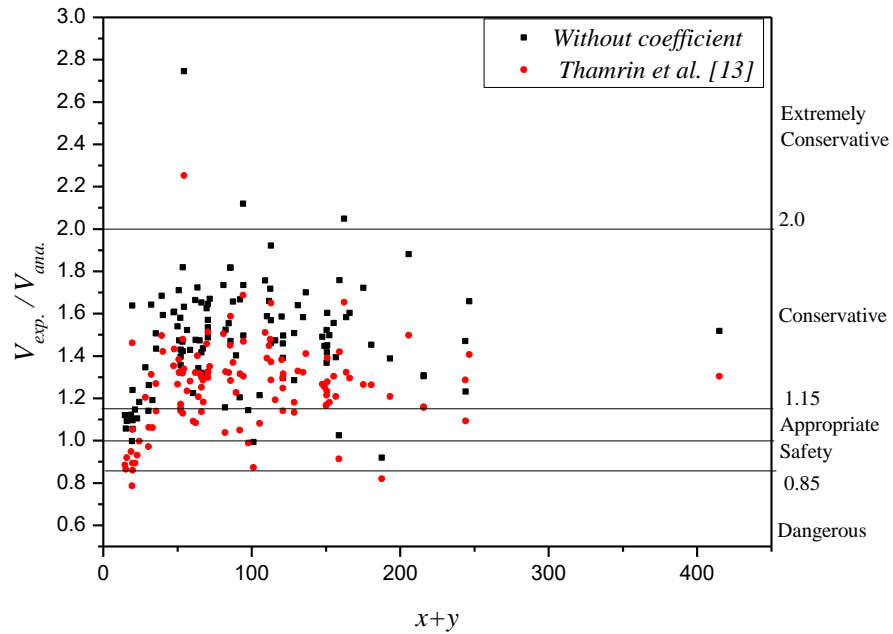
a) Thamrin et al. [13] suggestion
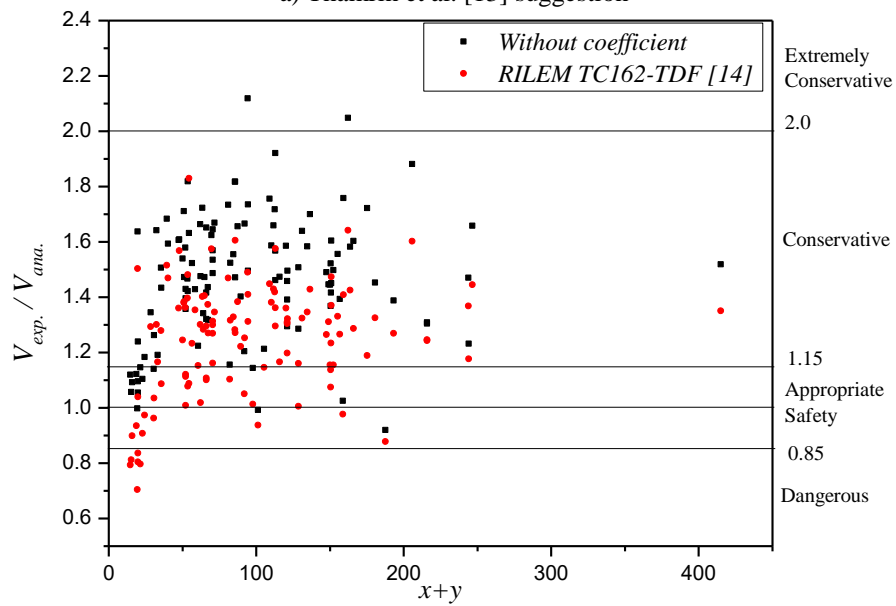
b) Rilem TC162-TDF [14] suggestion

Figure 5: Effects of flange on the load carrying capacity according to Thamrin et al. [13] and RILEM TC162-TDF [14] recommendation.

Figure 6: Distribution of the variables used in data base (DB)

Figure 7: Values of the experimental *vs.* analytical ratio for the T-cross section beams of the data base (

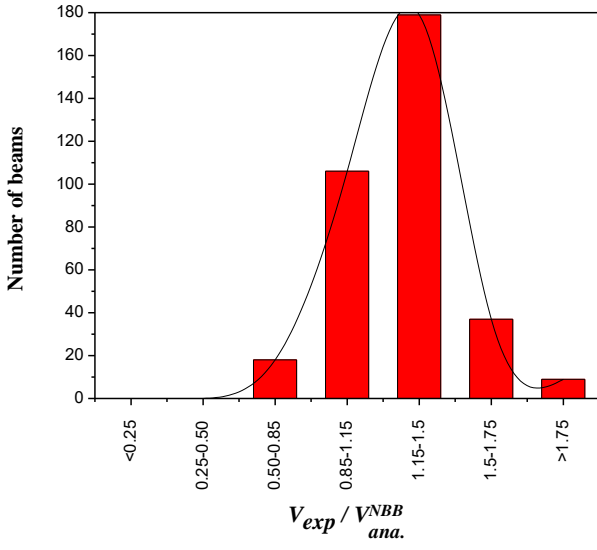$$x + y = \frac{\bar{\sigma}_{st}}{f_c'} + \frac{200000 \times \rho_{sl}}{f_c'} \times (\frac{b_w}{d}) \,)$$

Figure 8: Values of the experimental *vs.* analytical ratio for the analyzed approaches, considering the results from the collected data base ($x + y = \dfrac{\bar{\sigma}_{st}}{f_c'} + \dfrac{200000 \times \rho_{sl}}{f_c'} \times (\dfrac{b_w}{d})$))

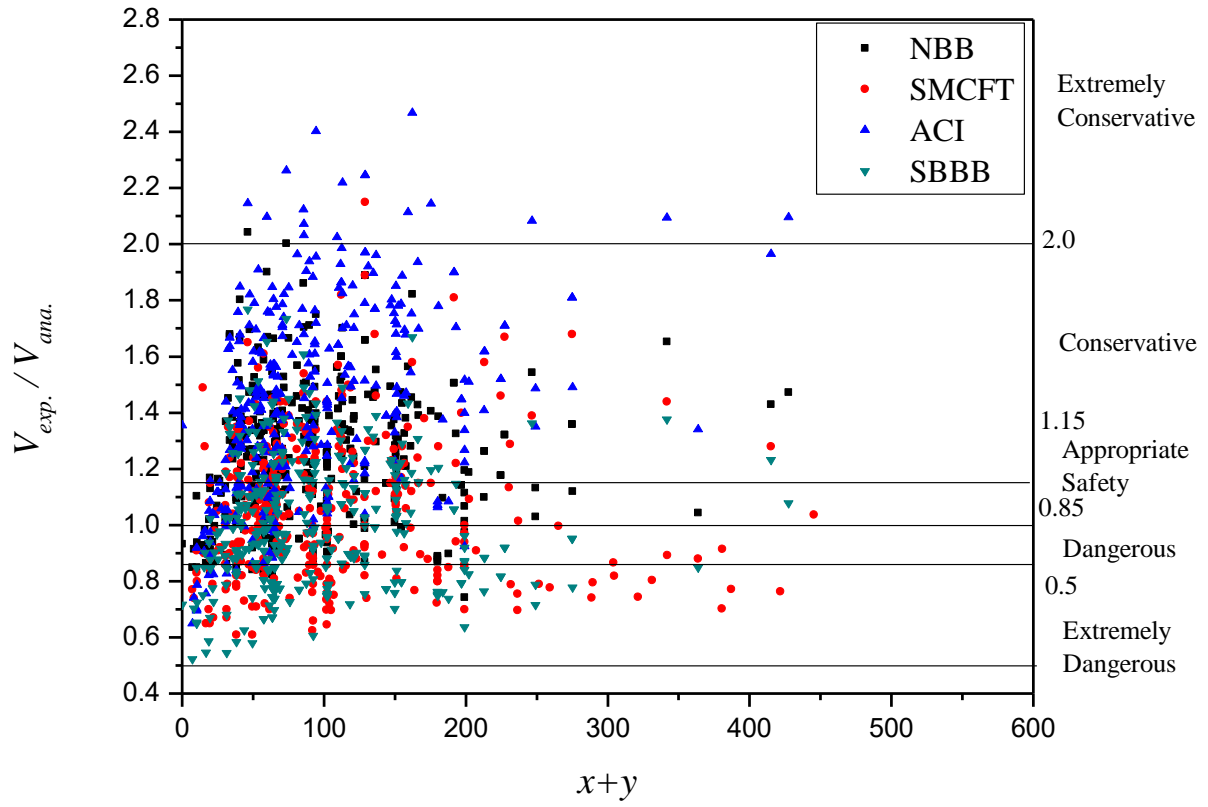Figure 9: Distribution of the results for different models.

Figure 10: Values of the experimental *vs.* analytical ratio, considering the results from the RDB
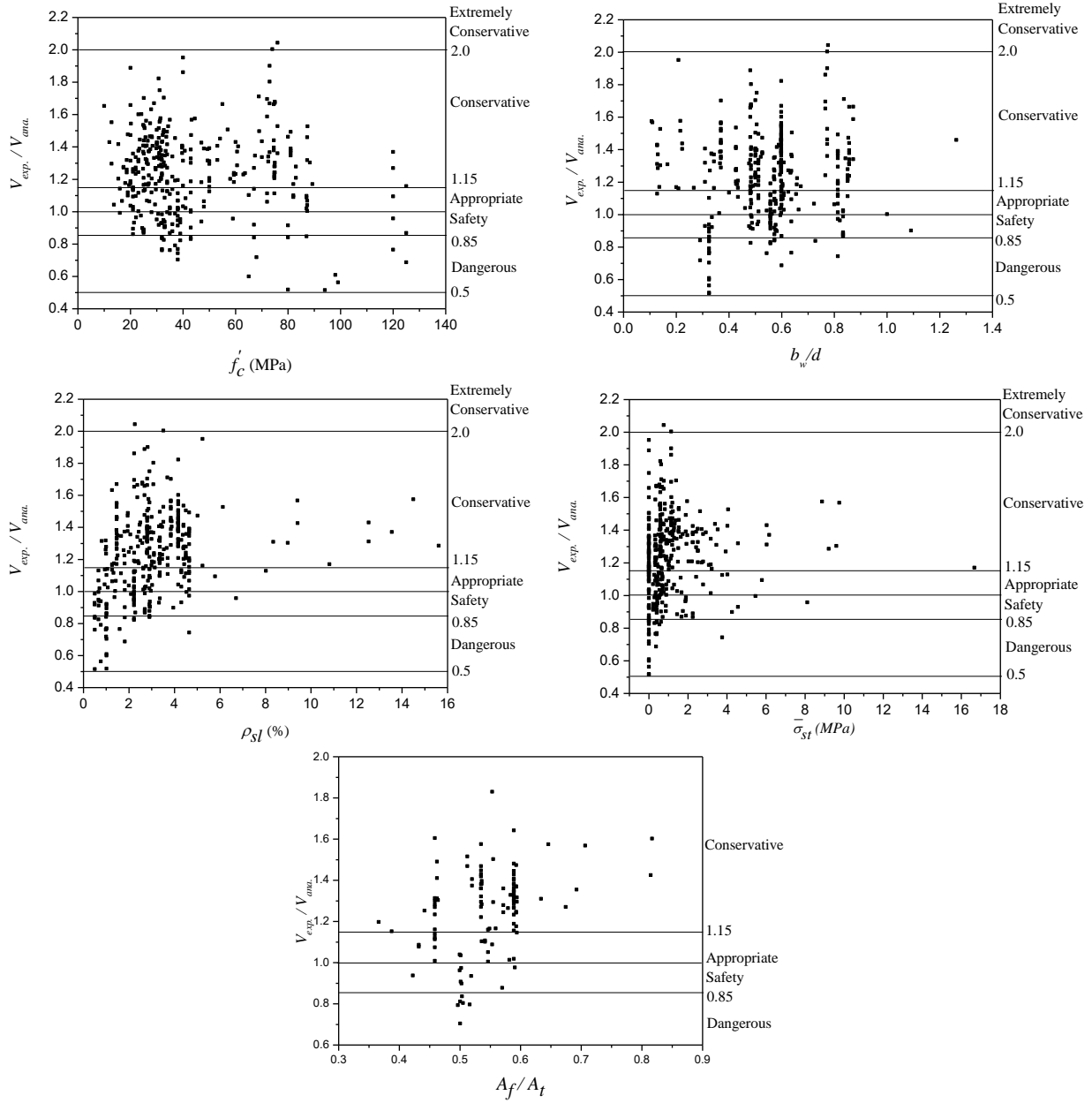
Figure 11: The ratio between the predicted and experimental shear strength values with respect to the $f_c^{'}$, d, ρ_{sl}, $\bar{\sigma}_{st}$, b_w, and A_f / A_t